TECHNISCHE UNIVERSITÄT WIEN

UHV techniques and Model Catalysis

1. Motivation and basics
2. Characterization methods
3. In situ spectroscopy on model catalysts
4. Molecular level case studies

1. Motivation

Why model systems?

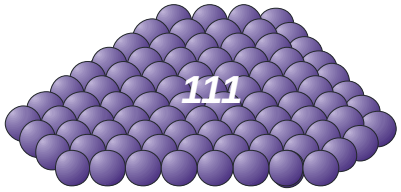

Use of **surface science approach** for new insights in catalysis

- surface chemistry, surface physics
- surface science toolbox → often **UHV** based
- **reduced complexity** compared to real catalysts → single crystals

Goals

- answering specific fundamental questions, looking at elementary steps
- help in assignment of bands, peaks, effects, etc.
- bridge/interface to simulation and DFT calculations

Challenges

- Cleanliness/contaminants
- Complex and expensive UHV techniques and setups
- Sensitivity (low surface area)

Nobel Prize 2007 in Chemistry

Pioneer in model catalysis

Gerhard Ertl
(Fritz Haber Institute Berlin)
for his studies of
Chemical Processes at Solid Surfaces

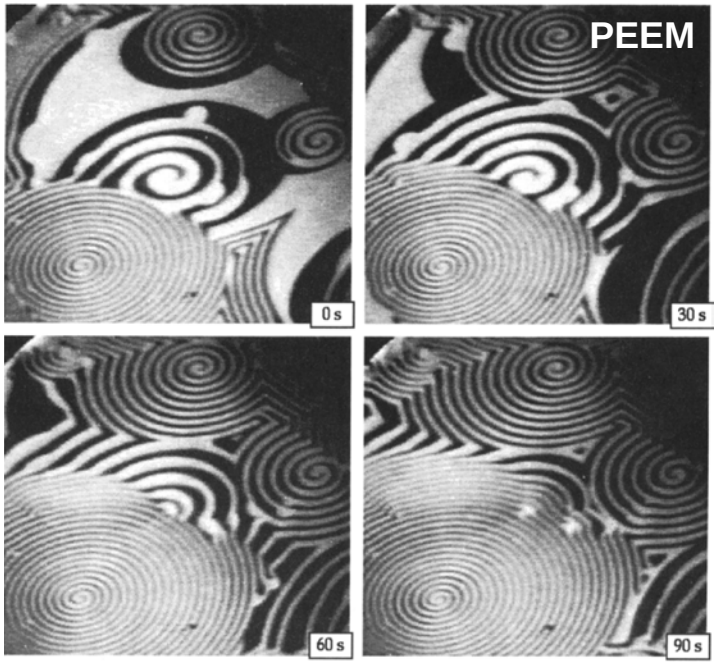

Oscillatory Surface Reactions:
CO oxidation on Pt(110)

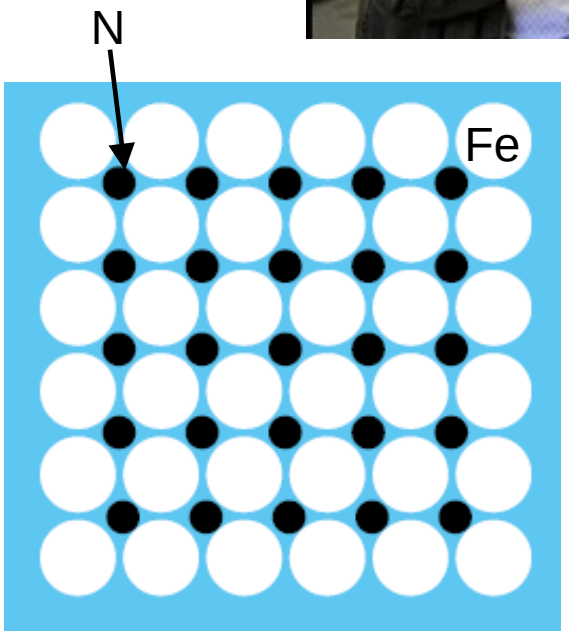

$$H_2 \rightleftharpoons 2\,H_{ad}$$

$$N_2 \rightleftharpoons N_{2,ad} \rightleftharpoons 2\,N_s$$

$$N_s + H_{ad} \rightleftharpoons NH_{ad}$$

$$NH_{ad} + H_{ad} \rightleftharpoons NH_{2,ad}$$

$$NH_{2,ad} + H_{ad} \rightleftharpoons NH_{3,ad}$$

$$NH_{3,ad} \rightleftharpoons NH_3$$

Ammonia Synthesis on Fe(100)

General Objectives in catalysis

- **Identification of the active sites**
- **Identification of reaction mechanism**

→ **Improve catalysts and processes on a rational basis**

Challenges

- Materials complexity:

  composition

  dynamics under reaction conditions

- Surface species:

  spectators, intermediates, poisons, …

  different configurations/geometries of adsorbates

→ **need for well defined + clean samples**

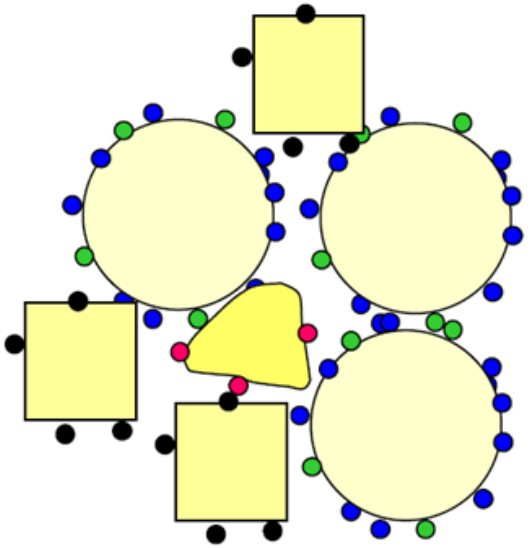

● Active site (for a particular reaction) one or more atoms in a particular configuration

Hugh Scott Taylor
Proc. Roy. Soc. A108, 105 (1925)

Catalyst Preparation

Impregnation of Microcrystalline supports

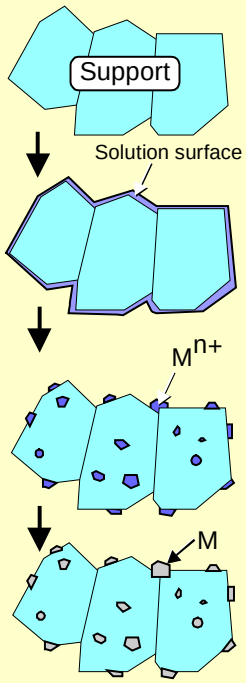

1. Support: aggregate of microcrystalline oxide (Al_2O_3, SiO_2, TiO_2, CeO_2, MgO, ...)
2. Impregnation with solution of the metal precursor, e.g. H_2PtCl_6, $[Pt(NH_3)_4](OH)_2$ $Rh(NO3)_3$, $RhCl_3$, $Rh(acac)_3$
3. Drying at ~353 K and/or calcination up to 773 K: particles of the metal precursor (storage)
4. Reduction in flowing hydrogen: 60 cc/min, Tred: 473 - 873 K
5. Activation in O_2 (~ 673 K) and H_2 (373 - 573 K)

activity and selectivity depend on:

metal precursor ($PdCl_2$, $Pd(NO_3)_2$, etc)

support oxide nature and „grade“

details of synthesis and processing, activation etc.

(on everything and even more …)

→ **need for well defined + clean samples**

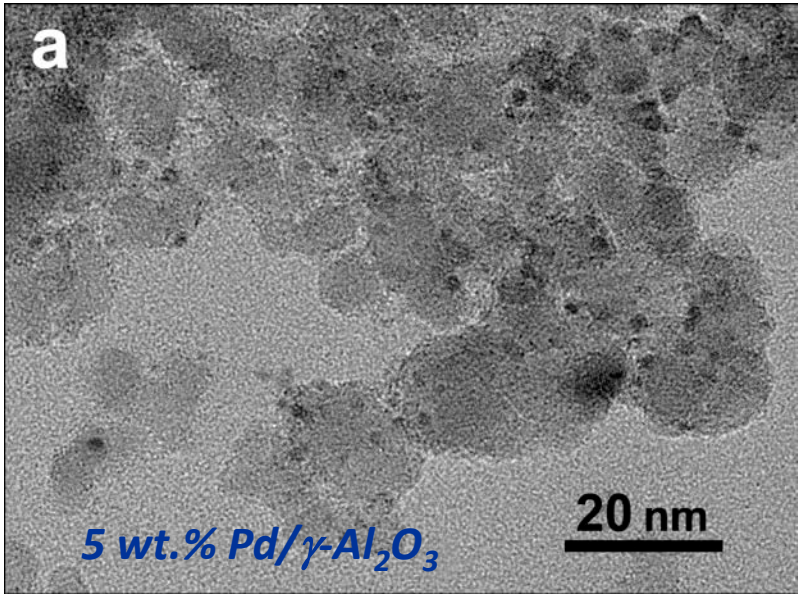

Example for effect of preparation residues:

Hydrodechlorination of trichloroethylene (TCE) to ethylene

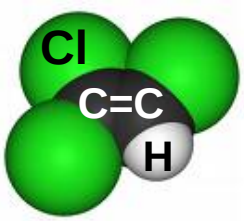

$$Cl_2C{=}CClH + H_2 \xrightarrow{Pt/CeO_2} C_2H_4 \ (+ C_2H_6)$$

precursor	synthesis	activation	C_2H_4 selectivity
H_2PtCl_6	impregnation	ox-red	high
$Pt(acac)_4$	impregnation	red	low

CeOCl phase decomposed by ox-red –
oxygen vacancies –
active sites for C-Cl cleavage –
Pt dissociates H_2 and regenerates clean surface

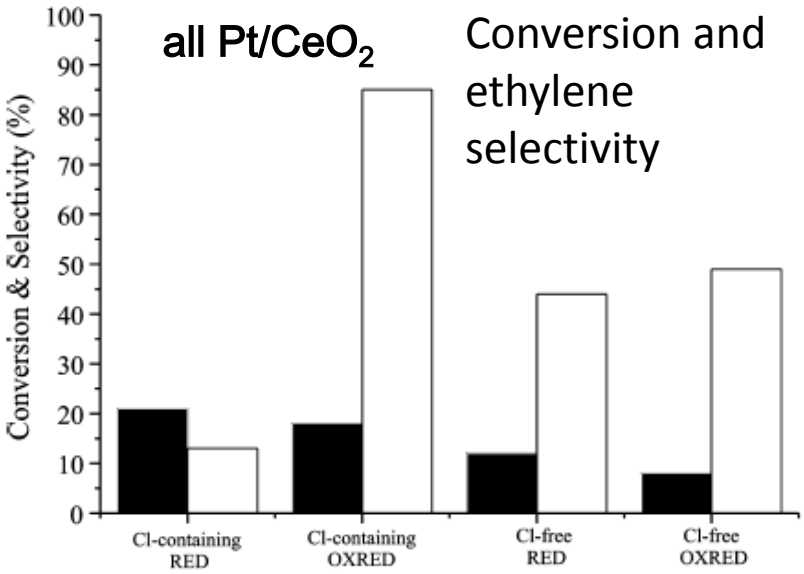

N. Barrabes, K. Föttinger, A. Dafinov, F. Medina, G. Rupprechter, J. Llorca, J.E. Sueiras, Applied Catalysis B: Environmental 87 (2009) 84

The surface: What does a real surface look like?

Even a single crystal surface has some defects!
Sites/atoms: terraces, edges, step edges, kinks, adatoms, vacancies, corners….

STM image of a TiO_2 surface

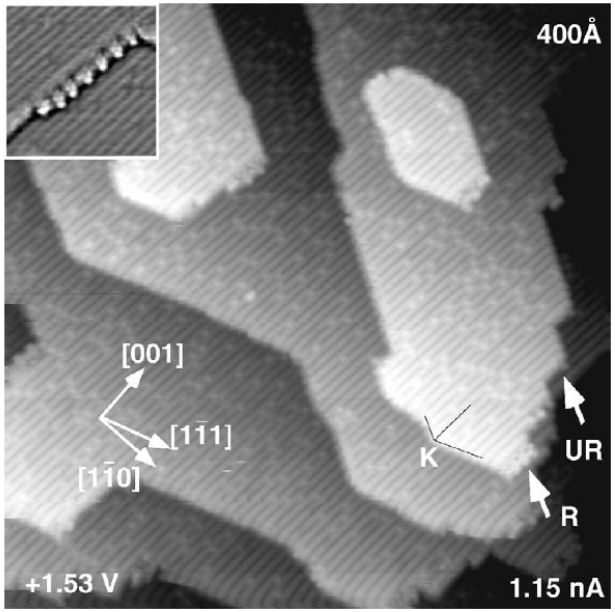

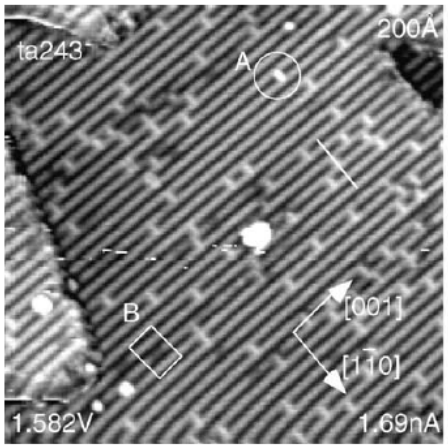

STM image (200 Å x 200 Å) of a TiO_2(1 1 0) surface showing point defects. Features labelled with „A“ have been assigned as oxygen vacancies.

Fig. 12. STM image of a clean stoichiometric TiO_2(1 1 0)-(1 × 1) surface after sputtering and annealing to 1100 K in UHV. The step structure is dominated by step edges running parallel to $\langle 1\,\bar{1}\,1\rangle$ and $\langle 0\,0\,1\rangle$ directions. A kink site at a $\langle 1\,\bar{1}\,1\rangle$ step edge is marked with 'K'. Smooth ('UR') and rugged ('R'econstructed) $\langle 0\,0\,1\rangle$-type step edges appear with roughly equal probability and are marked with arrows. The inset shows a 100 Å × 100 Å wide image of a reconstructed step edge. From

U. Diebold, Surf. Sci. Rep. 48 (2003) 53

The surface: What does a real surface look like?

Even a single crystal surface has some defects!
Sites/atoms: terraces, edges, step edges, kinks, adatoms, vacancies, corners….

Scheme of MgO surface: defects

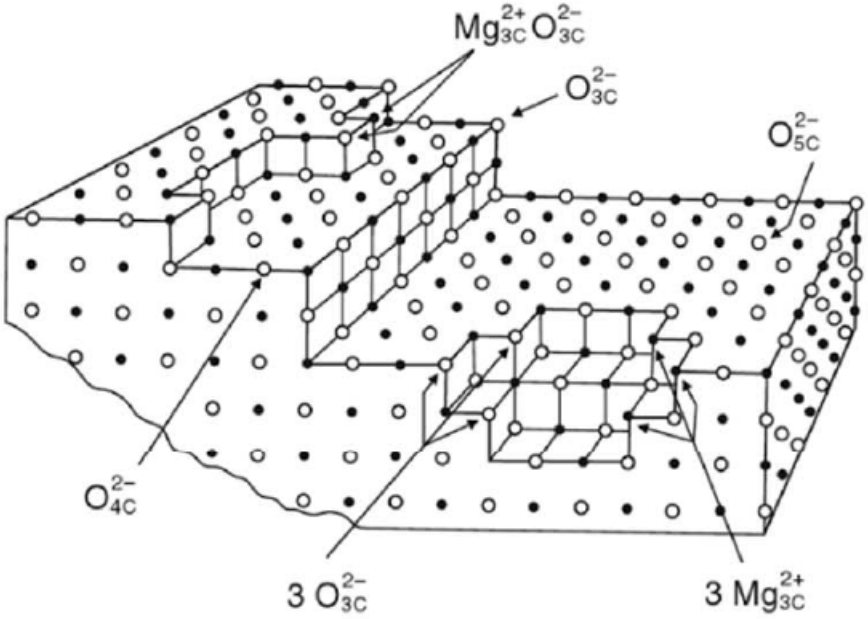

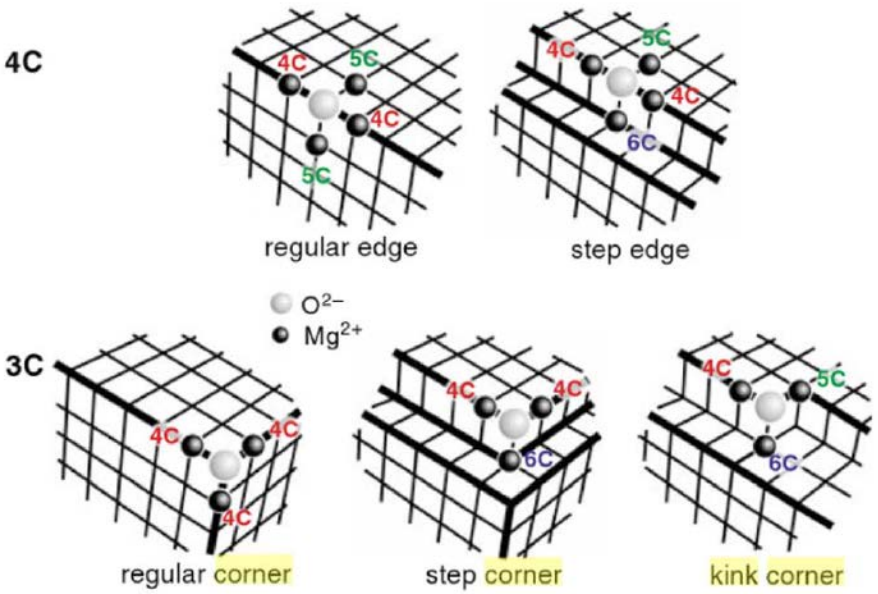

From „Defects at Oxide Surfaces“, eds. Jacques Jupille, Geoff Thornton
Springer

Types of model systems

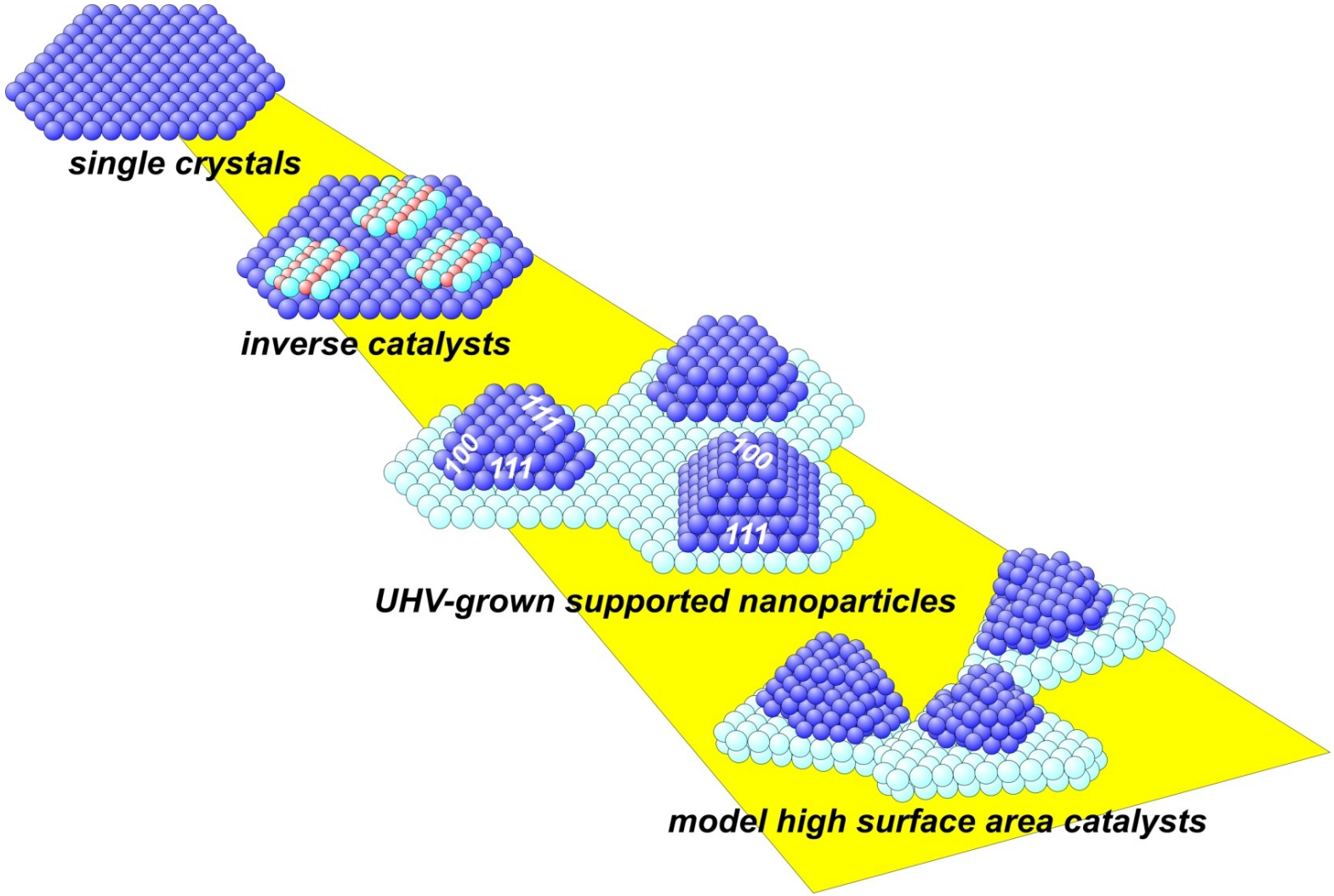

G. Rupprechter, C. Weilach
J. Phys.: Condens. Matter 20 (2008) 184019

Model Catalysts:

single crystal surfaces (e.g. Pd(111))

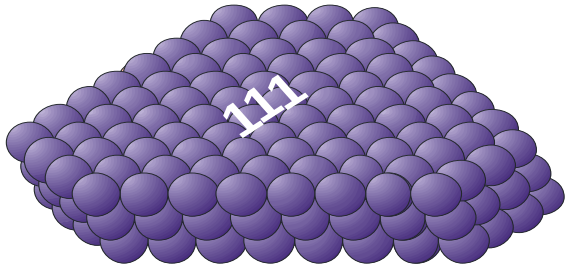

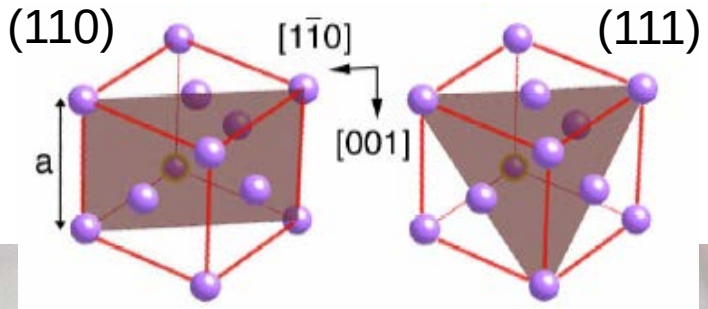

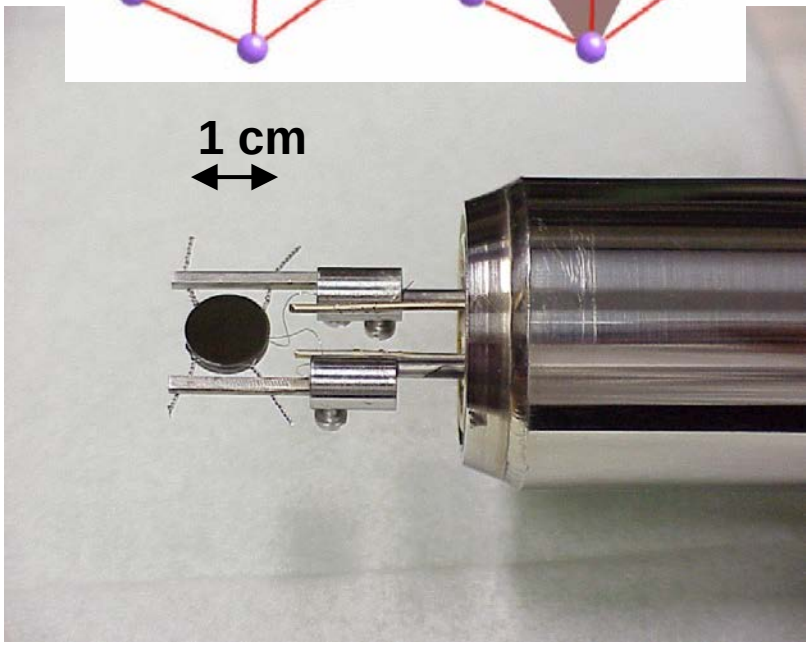

nanoparticles (e.g. $Pd/Al_2O_3/NiAl(110)$)

100 x 100 nm

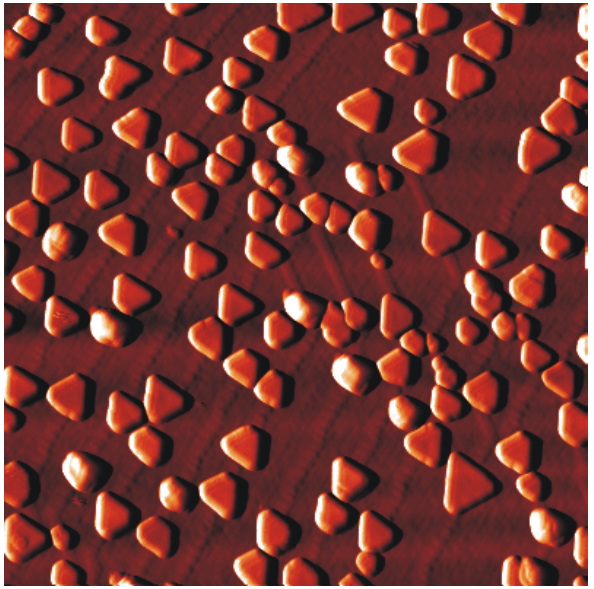

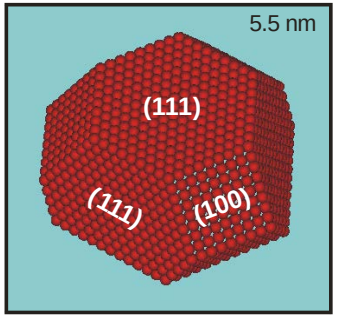

Why nanoparticles ? Nanosize Effects

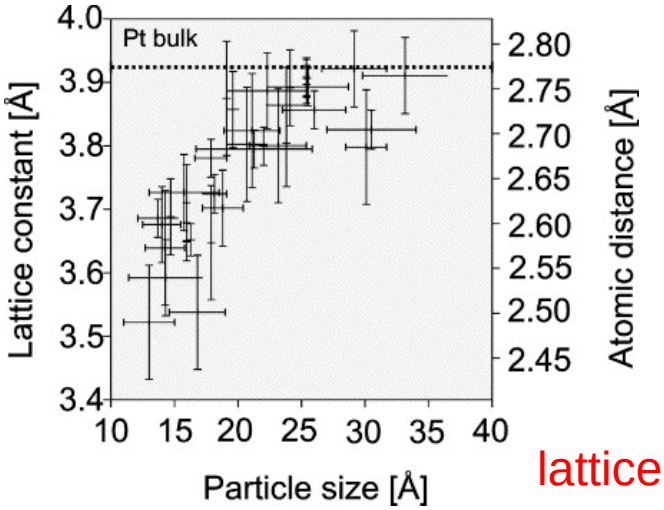

1

lattice parameter

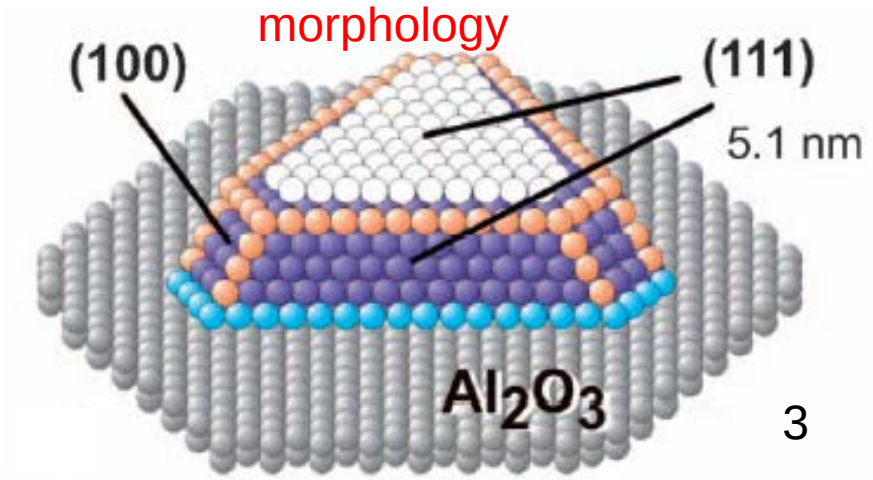

3

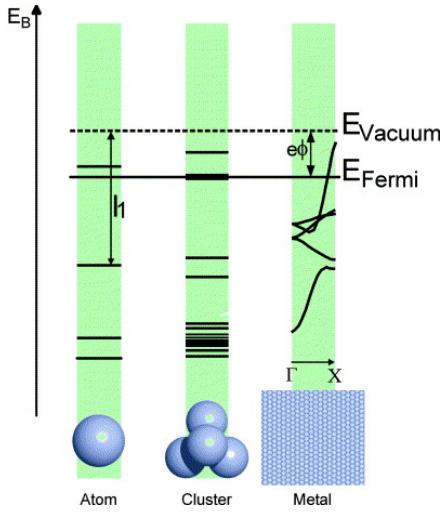

2

electronic structure

100-50-83-50-100 % Pt

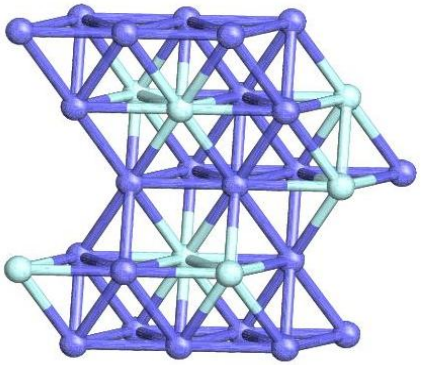

Pt_3Ni(111)
(surface segregation of Pt)

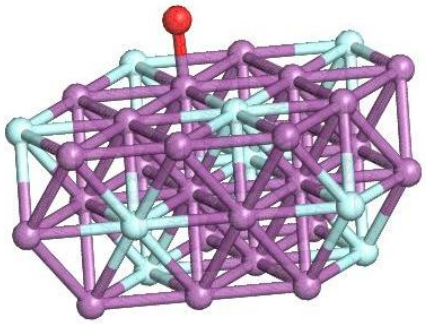

4

Pt_3Ni clusters
(no surface segregation)

composition

H.-J. Freund, Surface Science 500 (2002) 271

Gauthier et al. 1992
T. Jacob, W. A. Goddard III, JPC-B, 108, 8311 (2004)

Why nanoparticles ? Particle size effects

impregnated (powder) catalysts

structure sensitivity - particle size effect

R. van Hardeveld & A. van Montfoort,

Staatsmijnen in Limburg, Geleen, NL (-> DSM)

Surf. Sci. 4 (1966) 396-430

"The Influence of Crystallite Size on the Adsorption of Molecular Nitrogen on Nickel, Palladium and Platinum"

N_2 adsorption occurs only on small Ni particles between 1.5 and 7 nm

assumption: chemisorptive and catalytic properties of a surface atom vary with the number and arrangement of its nearest neighbors (coordination number)

largest fraction of edge and step related sites from 1.8 to 2.5 nm

"... the results point to the necessity of considering the diameter of metal catalyst particles as a new parameter in catalysis research."

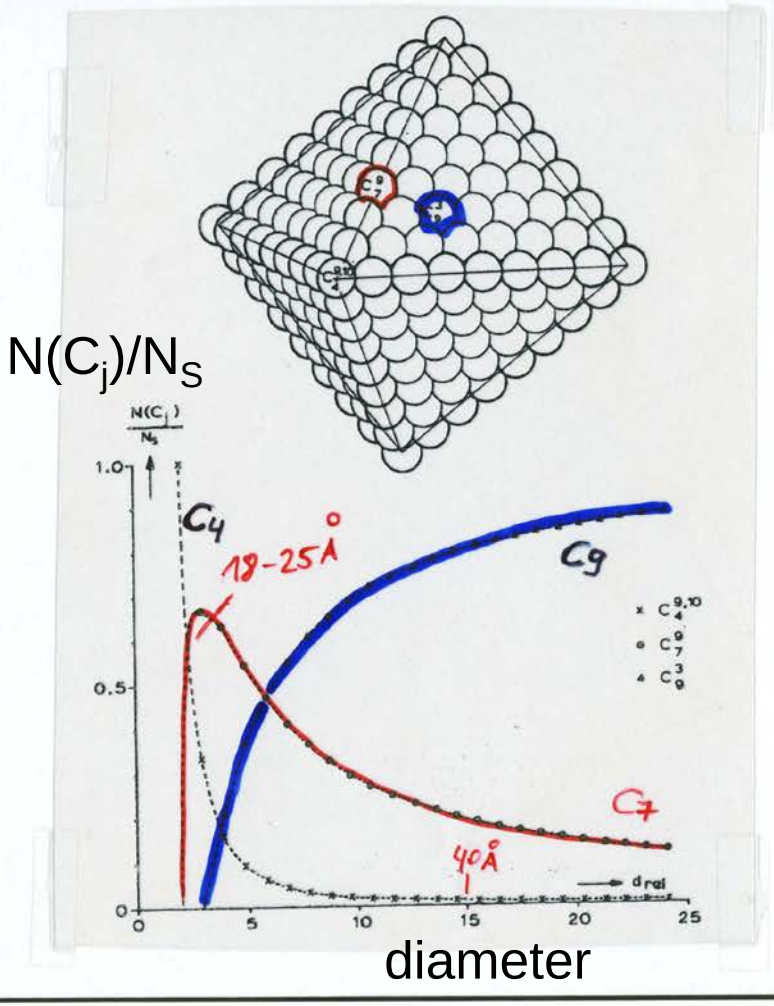

Why inverse catalysts ? Metal - support interaction

SMSI: electronic effect

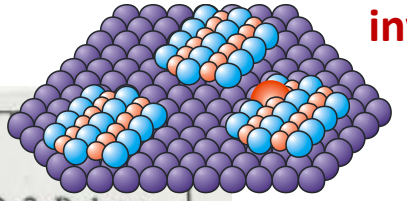

inverse catalysts

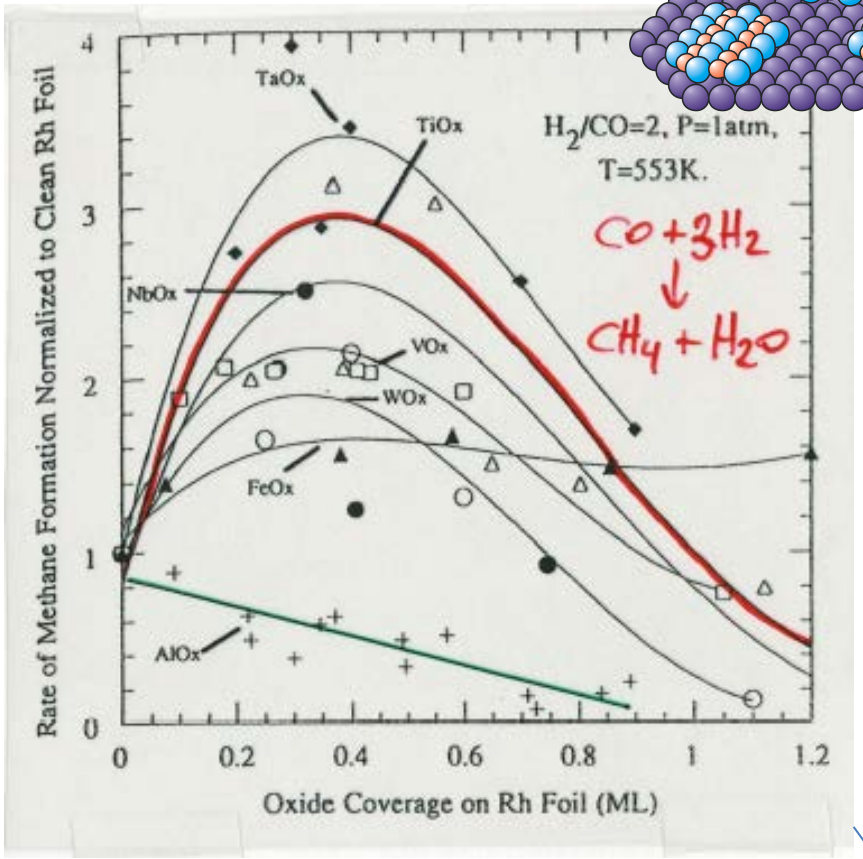

CO hydrogenation on Rh foil promoted by titania submonolayers

Bell, Somorjai et al., J. Catal. 106 (1987) 401

Hayek et al., Topics in Catal. 13 (2000) 55

SMSI: encapsulation

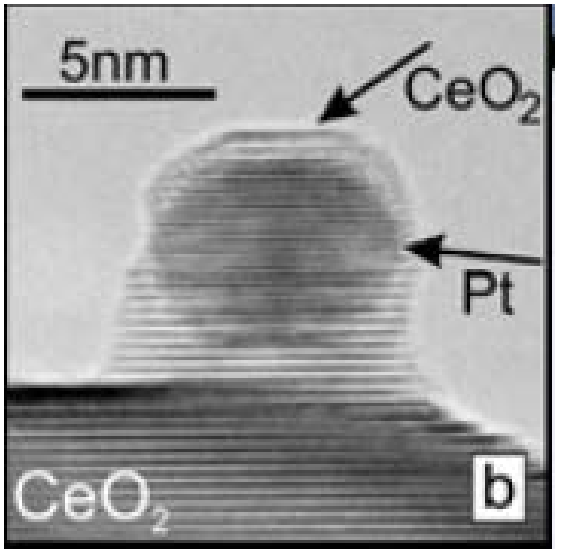

Compare TiOx (reducible oxide) → optimum loading, enhanced rate
and AlOx (non-reducible) → reduced active metal area

Preparation and cleaning

- Typically elaborate preparation and cleaning procedures
- Often freshly prepared surfaces for each experiment
- Cleaning by sputtering, annealing, gas treatments at high T

Sputtering:

- preparation: sputter deposition for thin films (eroding material from a target onto substrate)
- cleaning: bombardment of target by energetic gas ions (e.g. Ar^+) → surface atoms ejected

How long does the surface remain clean ? → depends on p and t

Langmuir:

- unit of exposure/dosage to a surface
- defined by multiplying gas pressure by exposure time
- 1 L corresponds to an exposure of 10^{-6} Torr during 1 s
- assuming the sticking coefficient is 1, 1 L leads to a coverage of about 1 monolayer

→ ***UHV (pressure range < 10^{-9} mbar) !*** (time for experiments in range of hours)

Example: how long does it take until the surface is covered with 1 ML assuming a sticking coefficient 1 at $p=10^5$ Pa, $p=100$ Pa, $p=10^{-8}$ Pa ?

UHV setup for model studies at TU Wien

Stainless steel UHV setup with flanges, UHV pumps, pressure gauges, …
Typically 10^{-10} to 10^{-11} mbar base pressure
Baking out

Tools and components:
-Preparation
-Characterization
-Sample manipulation
-Resistive heating

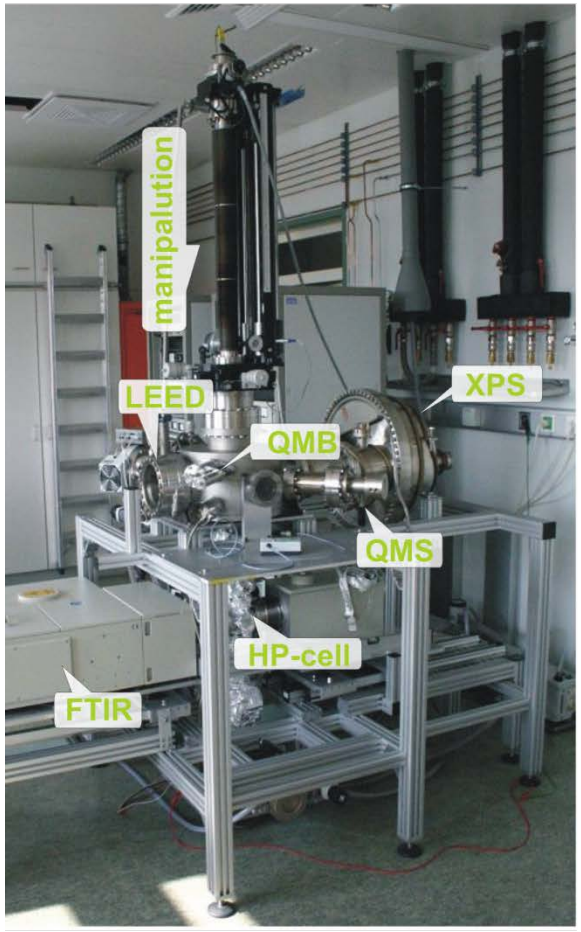

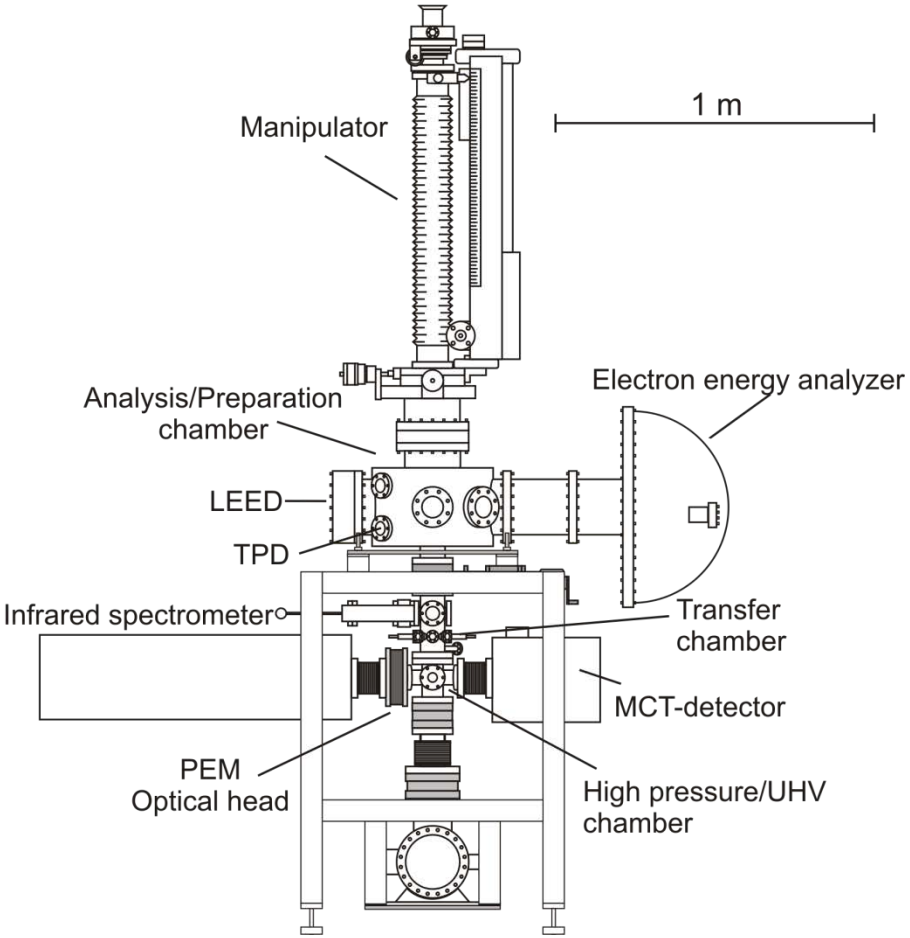

2. Characterization techniques

- Structure:

LEED, STM, AFM, LEIS

- Composition and adsorption sites:

XPS, AES, LEIS

TPD, IRAS, EELS

- Reactivity:

TPD, molecular beams, STM

XPS, AES, TPD, IRAS, EELS → see respective lectures

Surface Sensitivity when detecting electrons

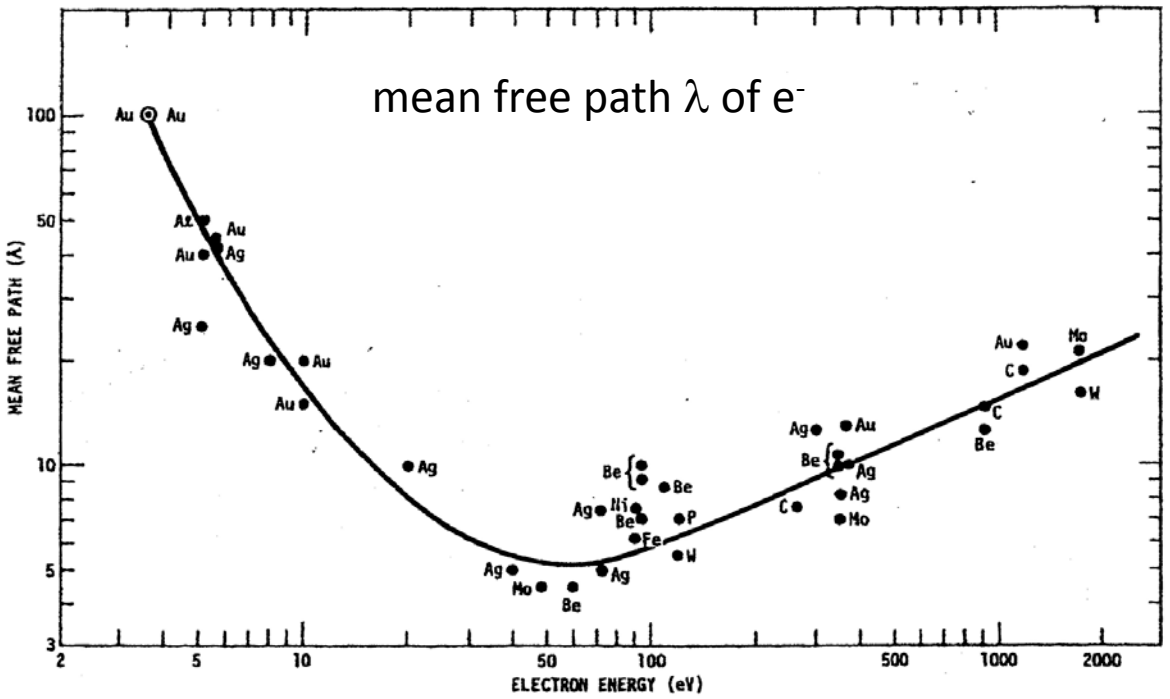

Figure 3.1: The mean free path of an electron depends on its kinetic energy and determines how much surface information it carries. Optimum surface sensitivity is obtained with electrons in the 25 - 200 eV range (from Somorjai, [16]).

for E_{kin} 15-1000 eV

λ = 1-2 nm

optimum: 50-250 eV –>
λ = 0.5 nm

95% of signal intensity originate from layer thickeness 3λ

50% from top layer (interface)

Surface Structure Analysis – Low Energy Electron Diffraction

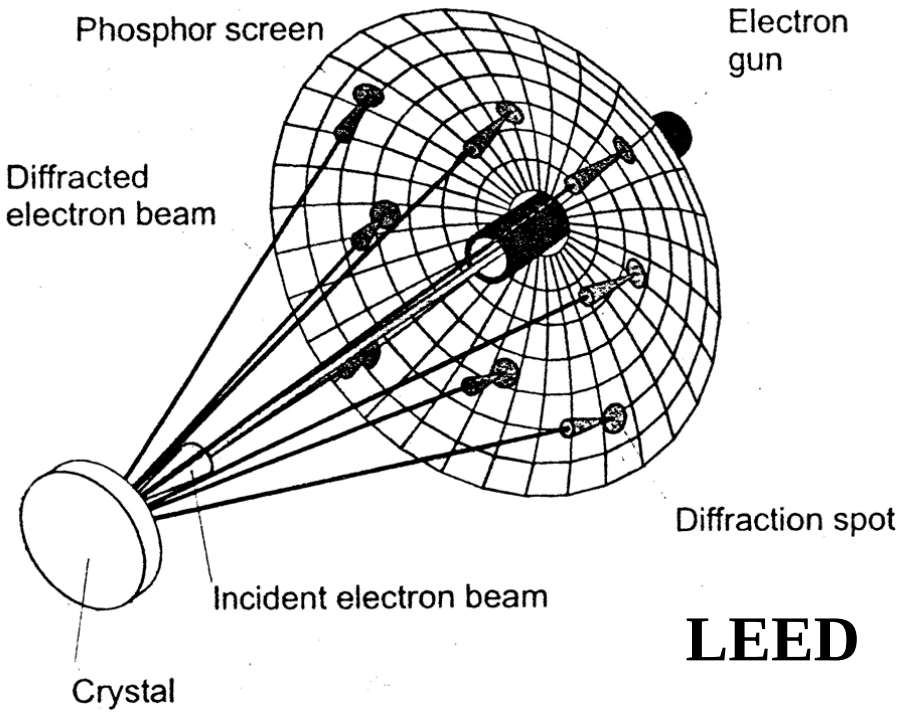

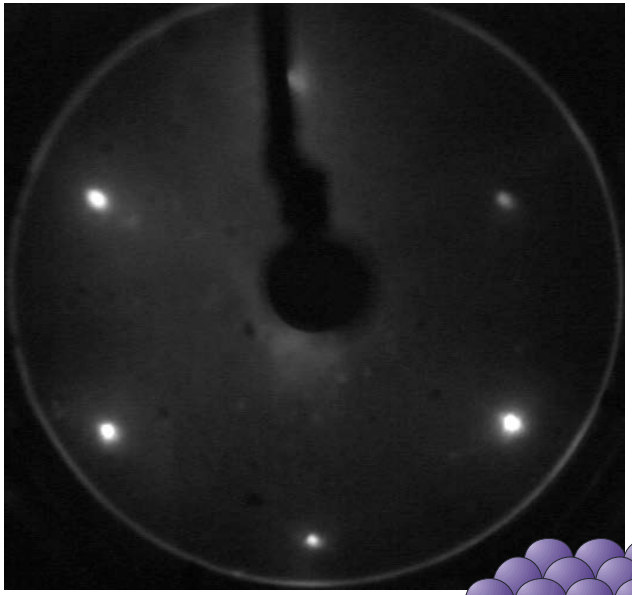

Pd(111)

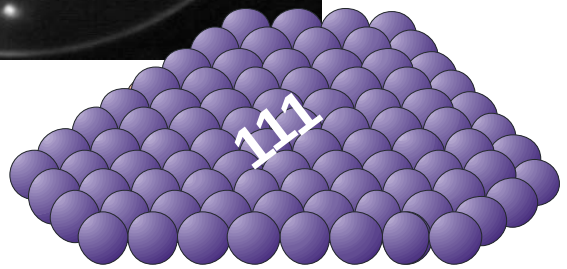

LEED

$n\lambda = a \sin\alpha$

collimated beam of low energy electrons (20–200 eV)
wavelength of 100 V electrons: ~1Å

LEED

- Surface structure and symmetry
- Reconstruction
- Structure of adsorbates

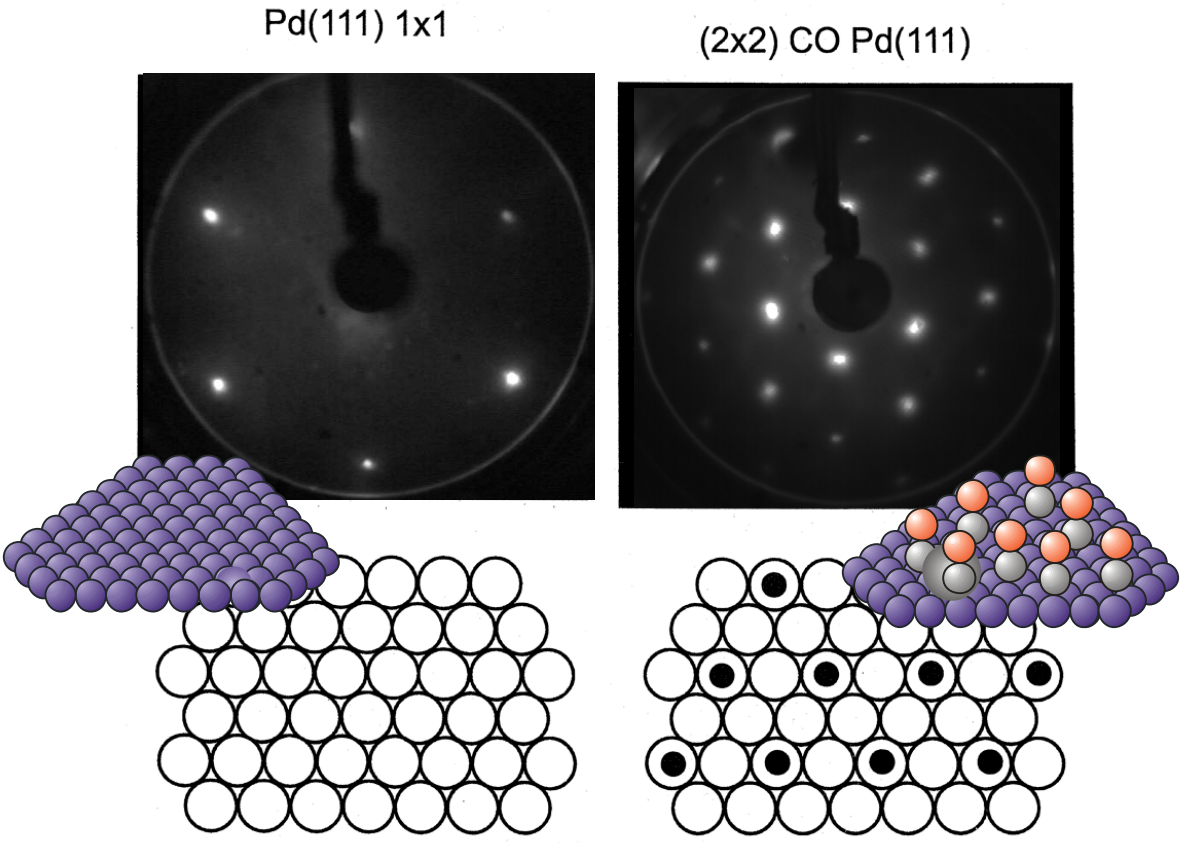

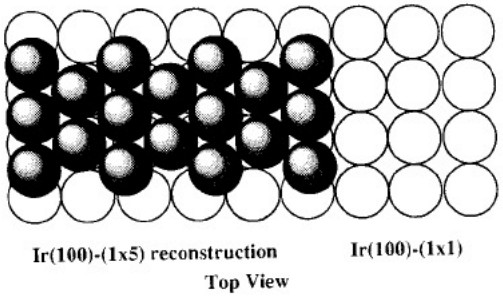

Figure 8. Top and side view of the Ir(100)-(1×5) surface reconstruction. The more open square (100) lattice is reconstructed into a close-packed hexagonal overlayer, with a slight buckling as shown in the side view.

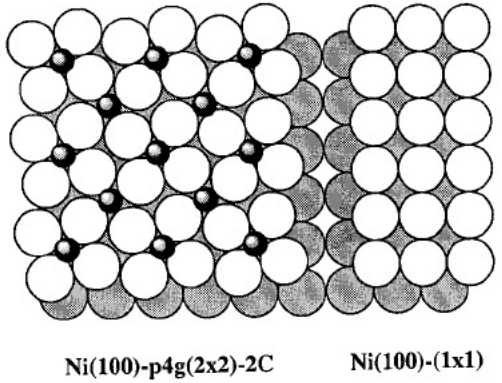

Figure 12. Carbon-chemisorption-induced restructuring of the Ni(100) surface.

Low-energy ion scattering spectroscopy (LEIS)

Ion stream directed at a surface
observation of the positions and energies of the ions that have interacted with the surface
→deduce information about relative positions of atoms in a surface lattice and their elemental identity → **structure and composition**

Ion source (mostly noble gases), optics (electrostatic lenses for focusing, collimation), sample manipulation (position, angle), detector (electrostatic analyzer), UHV pumps

Energy range: ca. 500 eV to 20 keV

unique in high sensitivity to the first surface layer

elastic collisions → energy and momentum conservation → determination of the mass of the scattering surface atom from energy of outgoing (scattered) ions

Low-energy ion scattering spectroscopy (LEIS)

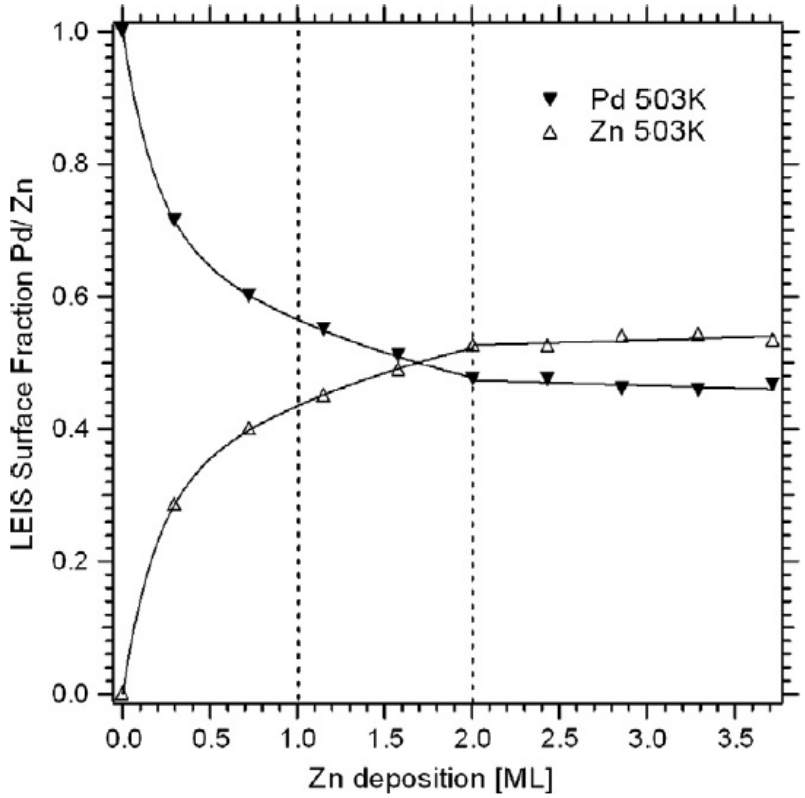

Fig. 2. LEIS-derived Pd:Zn surface composition on Pd foil after ~300 K Zn deposition and subsequent thermal annealing at 503 K.

→ follow surface alloy formation

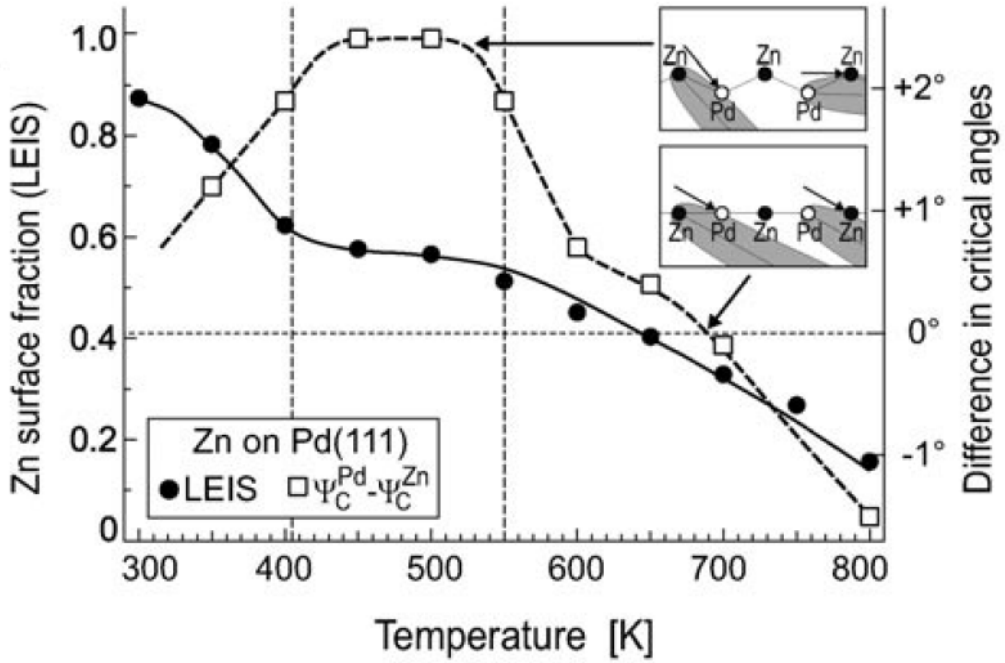

● Pd:Zn surface fractions derived from LEIS for Zn films deposited on Pd(111). ○ Difference in critical angles for backscattering of 5 keV Ne ions from Pd and Zn atoms. Inset: schematic side views of a corrugated and a non-corrugated (2x1) PdZn surface. Arrows and gray shadow cones indicate the critical angles where backscattering from Pd and Zn atoms, respectively, sets in.

C. Rameshan et al., Journal of Catalysis 276 (2010) 101.

C. Rameshan et al., Angew. Chem. Int. Ed. 49 (2010) 3224.

Scanning Tunneling Microscopy (STM)

Operating principle

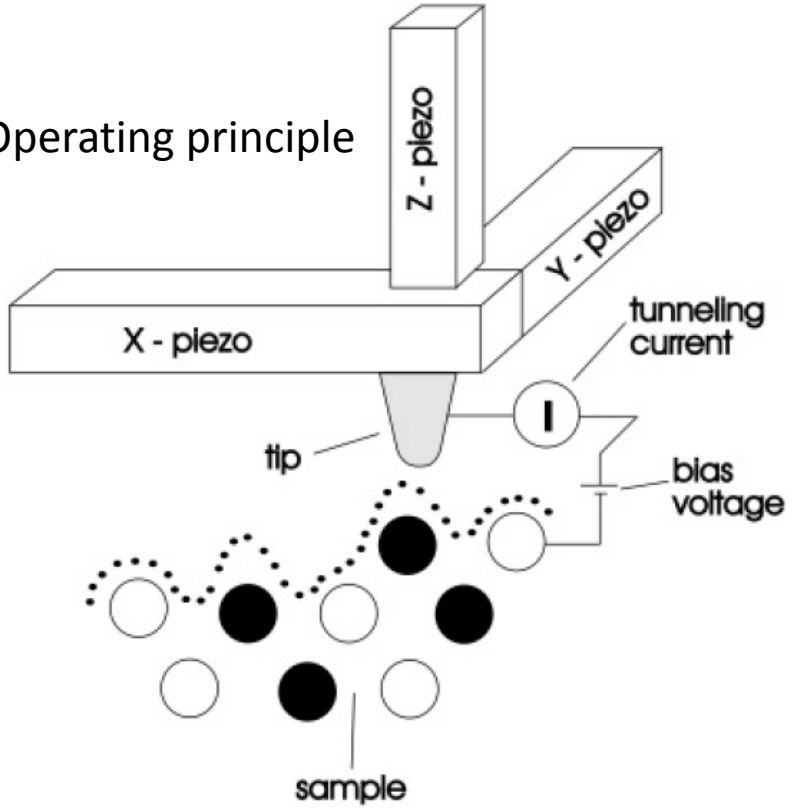

Energy level diagram

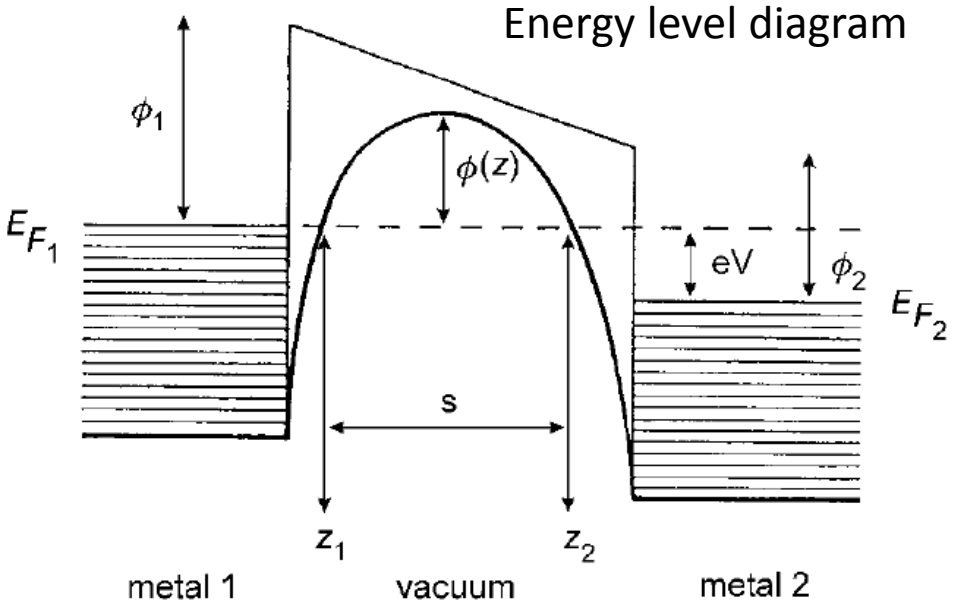

Φ …metals work function

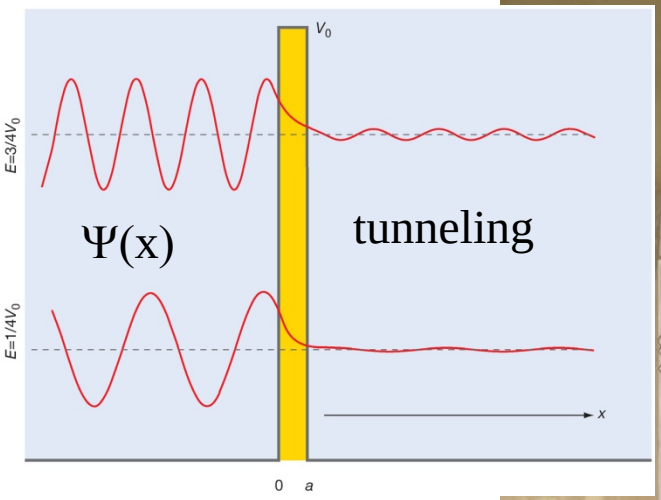

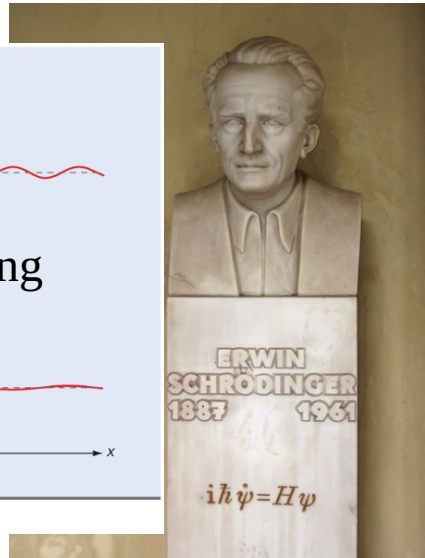

- distances typically 1 nm or less
- bias voltage of a few millivolts between tip and sample
- tunneling current a few nanoamperes

Surface and Thin Film Analysis: A Compendium of Principles, Instrumentation, and Applications. Edited by Gernot Friedbacher, Henning Bubert. 2011 Wiley-VCH

Scanning Tunneling Microscopy (STM)

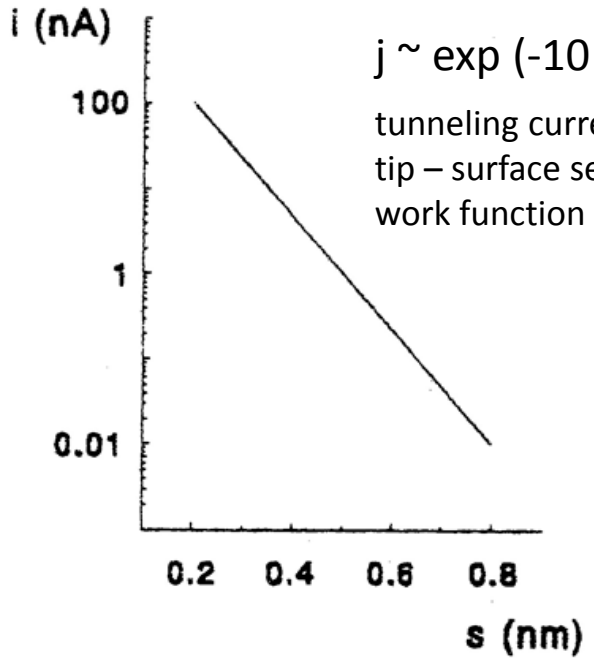

$j \sim \exp(-10\, s \sqrt{\Phi})$

tunneling current j (nA)
tip – surface separation s (nm)
work function Φ (eV)

Images of atoms/LDOS

Images or movies of processes e.g. chemical reactions

- exponential relationship tunneling current – tip-surface separation → extremely sensitive
- tunneling current depends on the electronic structure of the surface (**local density of states**)

- Image of individual atoms
- not only in UHV but also in various liquid or gas ambients
- at T ranging from near 0 K to a few hundred °C.
- well-defined planar and conducting surfaces needed

Scanning Tunneling Microscopy (STM)

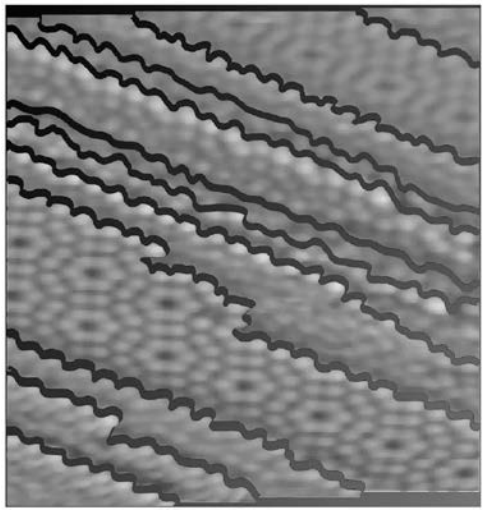

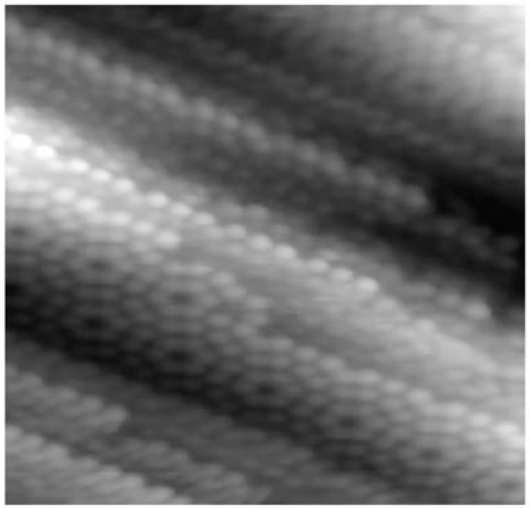

Si(111) surface

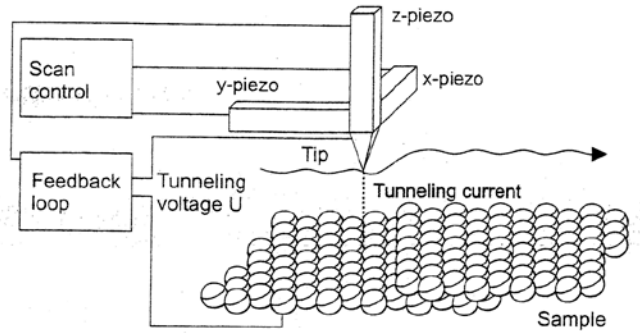

100 x 100 nm

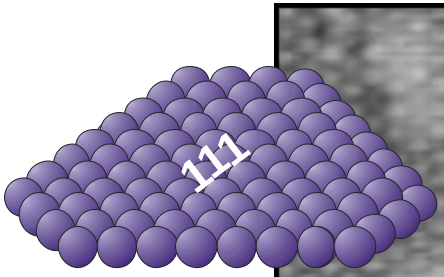

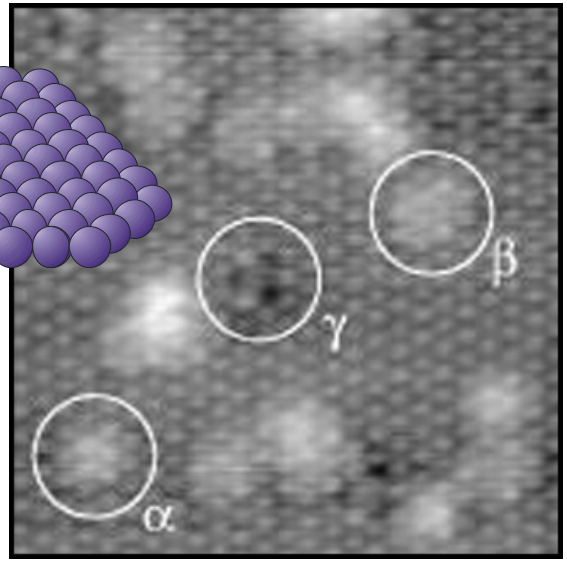

Pd(111)

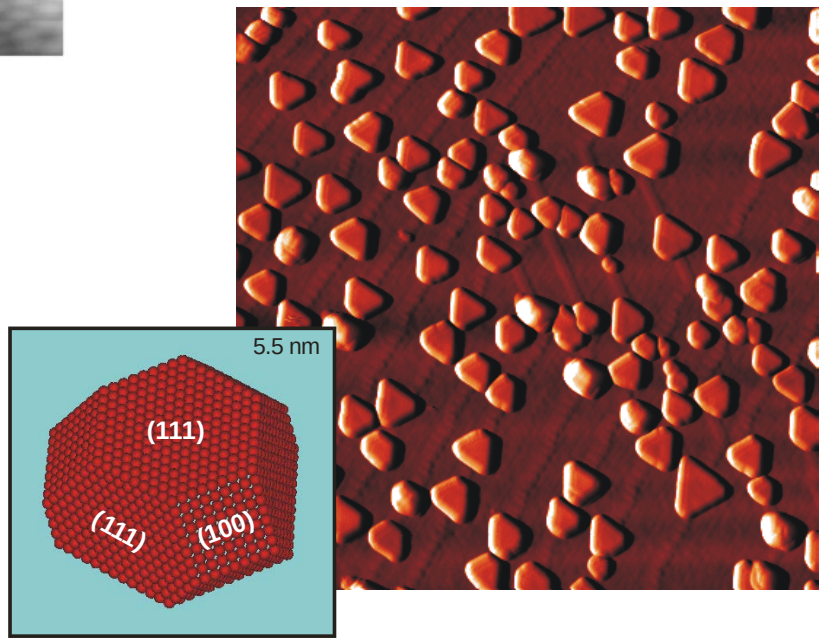

Pd nanoparticles on Al_2O_3

Example: following reacions and determining reaction parameters by STM: CO oxidation on Pt(111)

Wintterlin et al., Science 278 (1997) 1931.

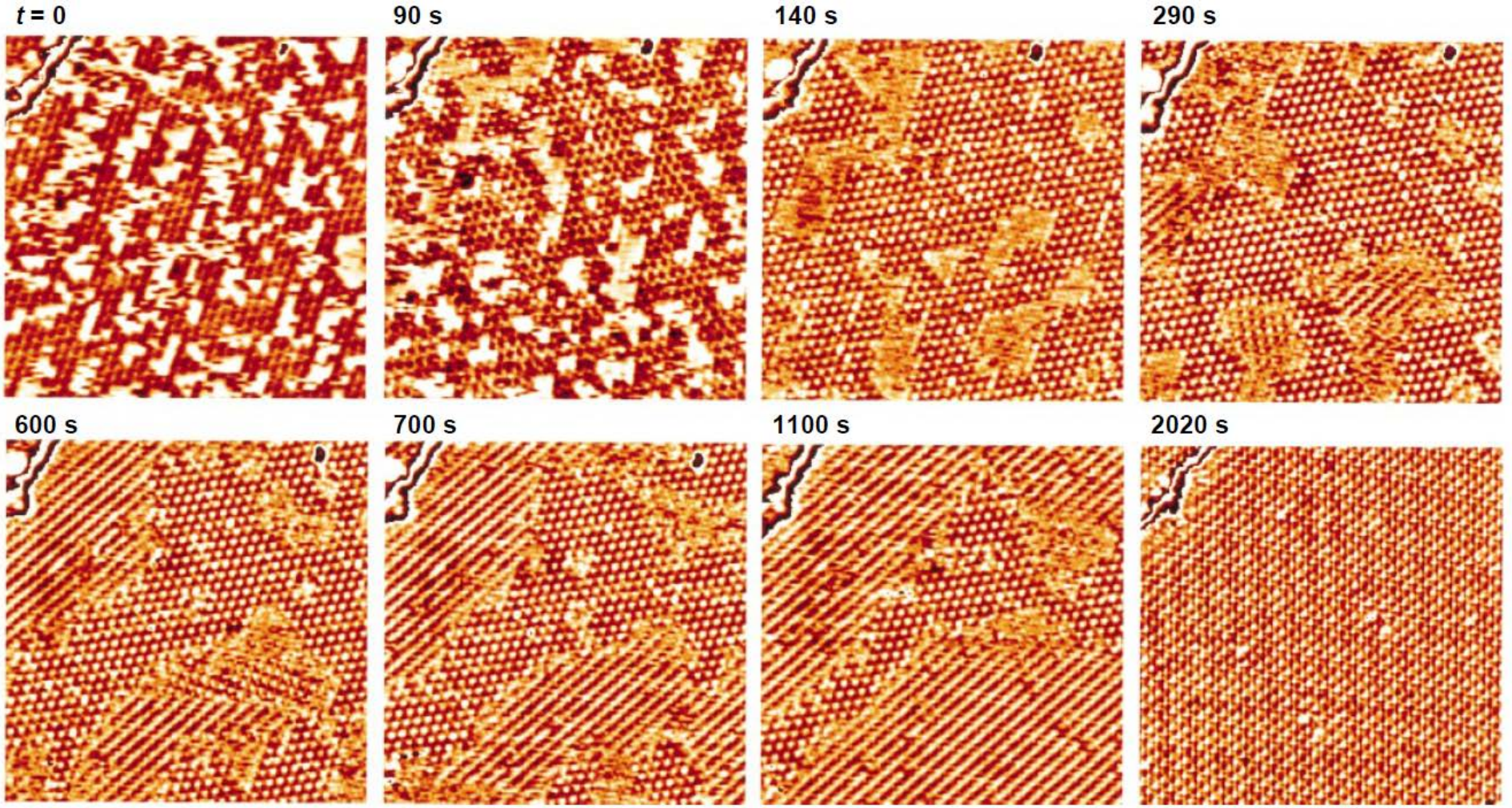

Fig. 1. Series of STM images, recorded during reaction of adsorbed oxygen atoms with co-adsorbed CO molecules at 247 K, all from the same area of a Pt(111) crystal. Before the experiment, a submonolayer of oxygen atoms was prepared (by an exposure of 3 Langmuirs O_2 at 96 K, a short annealing to 298 K, and cooling to 247 K), and CO was continuously supplied from the gas phase ($P_{CO} = 5 \times 10^{-8}$ mbar). At this pressure, the impingement rate of CO molecules is about 1 monolayer per 100 s, where the zero-coverage sticking coefficient on the empty and oxygen-covered surface is about 0.7 (*8*); the times refer to the start of the CO exposure. The structure at the upper left corner is an atomic step of the Pt surface. Image sizes, 180 Å by 170 Å; tunneling voltage (with respect to the sample), +0.5 V; tunneling current, 0.8 nA.

3. From UHV to in situ studies

- PMIRAS
- sum frequency generation (SFG)
- near ambient pressure (NAP)XPS
- high pressure STM

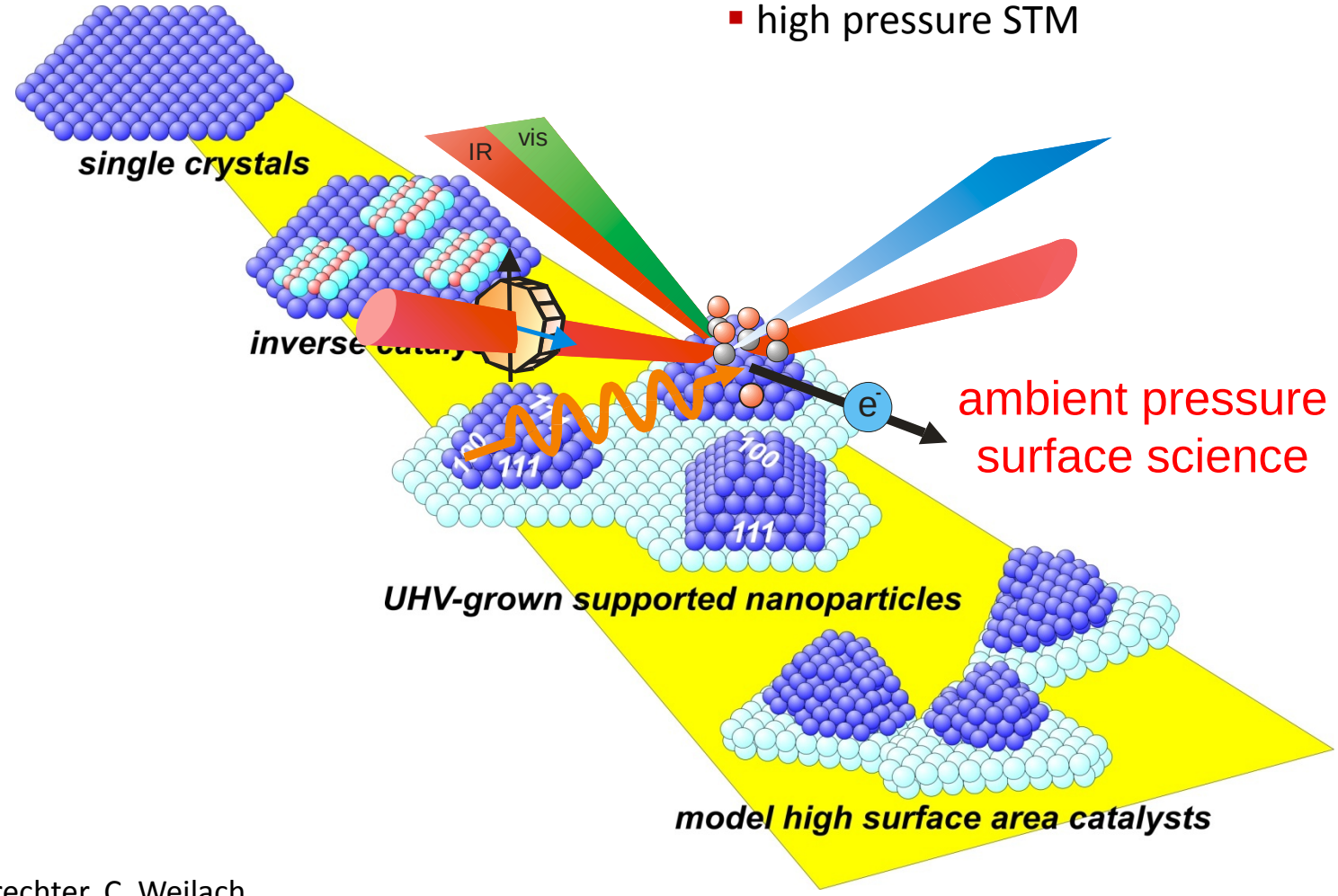

G. Rupprechter, C. Weilach
J. Phys.: Condens. Matter 20 (2008) 184019

Why in situ studies on model systems

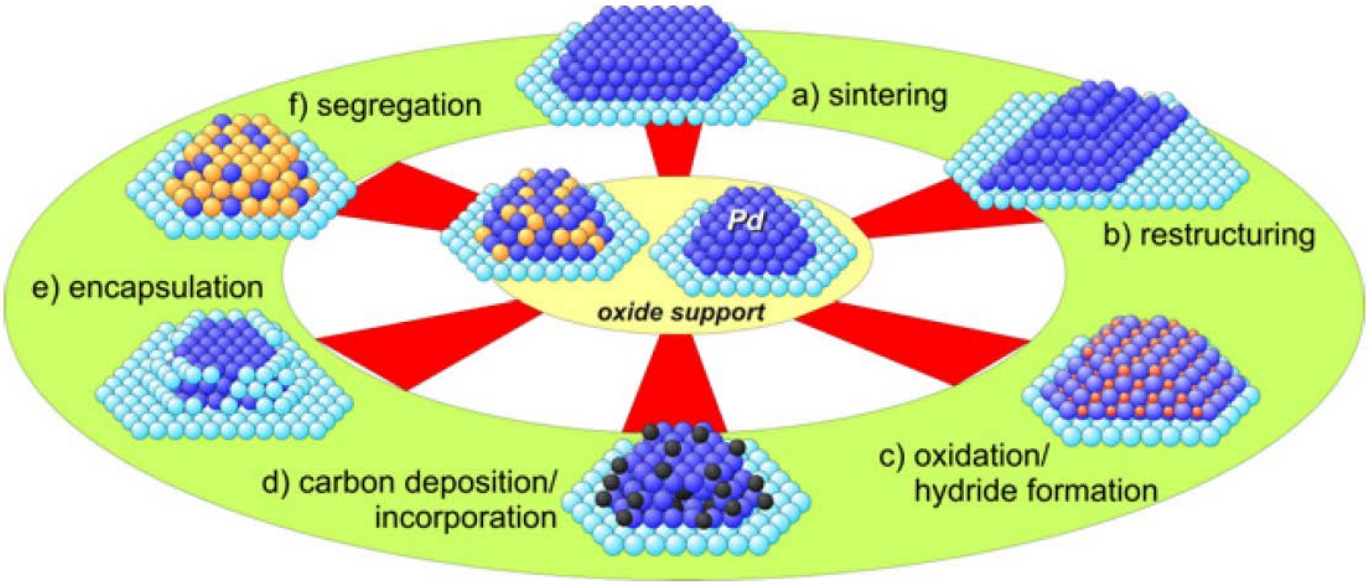

Figure 1. Illustration of structural and compositional changes that may occur during the transformation of catalysts from the 'as-prepared' to the 'active state': sintering and restructuring ((a), (b)), oxide/hydride formation and coking ((c), (d)), particle encapsulation (e) and surface segregation of bimetallic particles (see the text for details).

G. Rupprechter, C. Weilach
J. Phys.: Condens. Matter 20 (2008) 184019

Vibrational Spectroscopy on Model Catalysts

Polarization-Modulation Infrared Reflection-Absorption Spectroscopy (PM-IRAS)

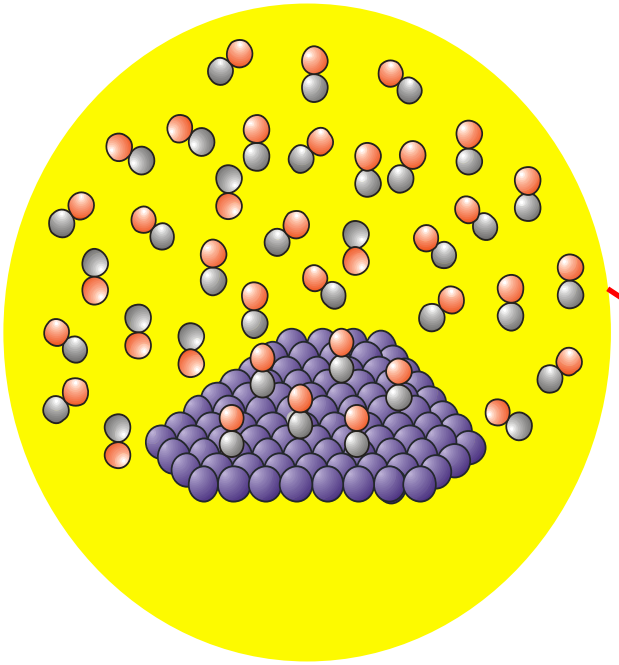

CO adsorbed
on Pd(111)
in 50 mbar CO

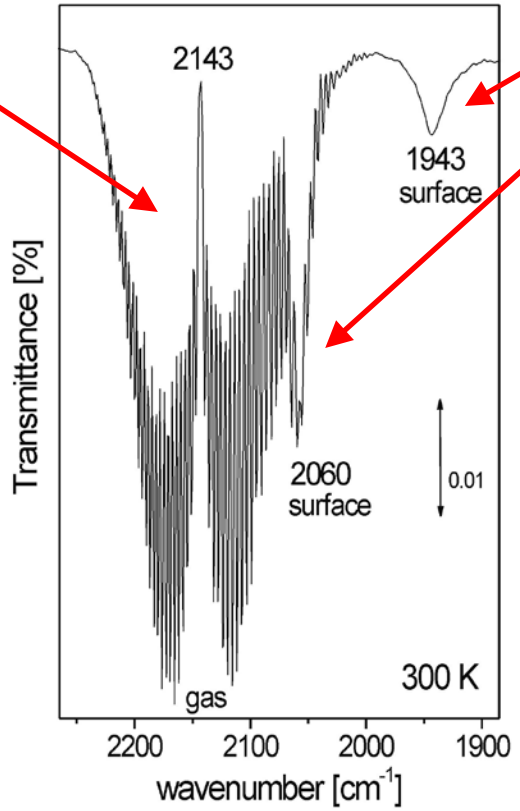

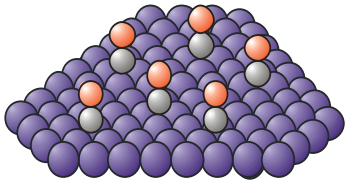

CO adsorbed
on Pd(111)
in ultrahigh vacuum

superposition of surface and
gas phase contributions

Vibrational Spectroscopy on Model Catalysts

Polarization-Modulation Infrared Reflection-Absorption Spectroscopy (PM-IRAS)

→ ***see lecture by Dr. Ferri***

PM-IRAS setup

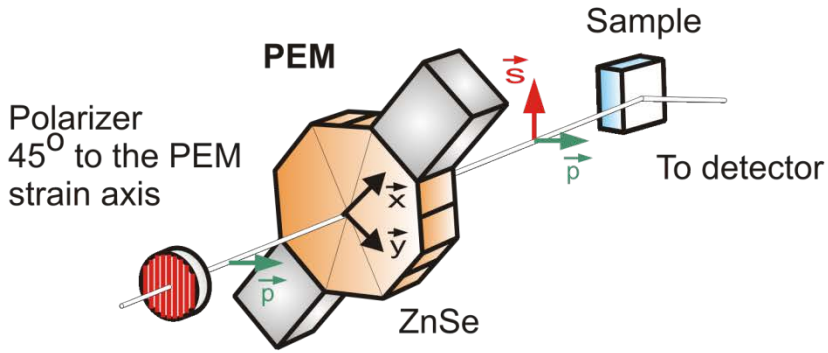

at metal surfaces:

p - polarization: gas phase + surface
s - polarization: gas phase

---

p – s: **SURFACE**

only those vibrations contribute to the absorption signal whose dynamic dipole moment possesses a non-zero component *perpendicular* to the metal surface: $(d\mu/dq)_\perp \neq 0$ *metal surface selection rule*
parallel component is screened by the metal electrons (s-polarized electric field is cancelled at a metal surface)

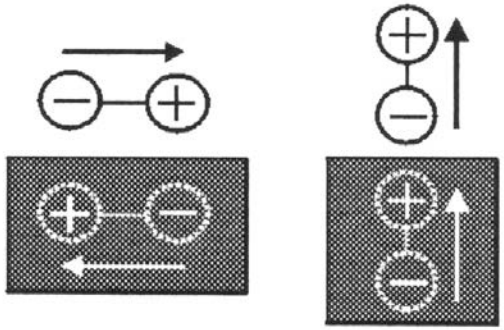

IR-vis Sum Frequency Generation (SFG) Laser Spectroscopy

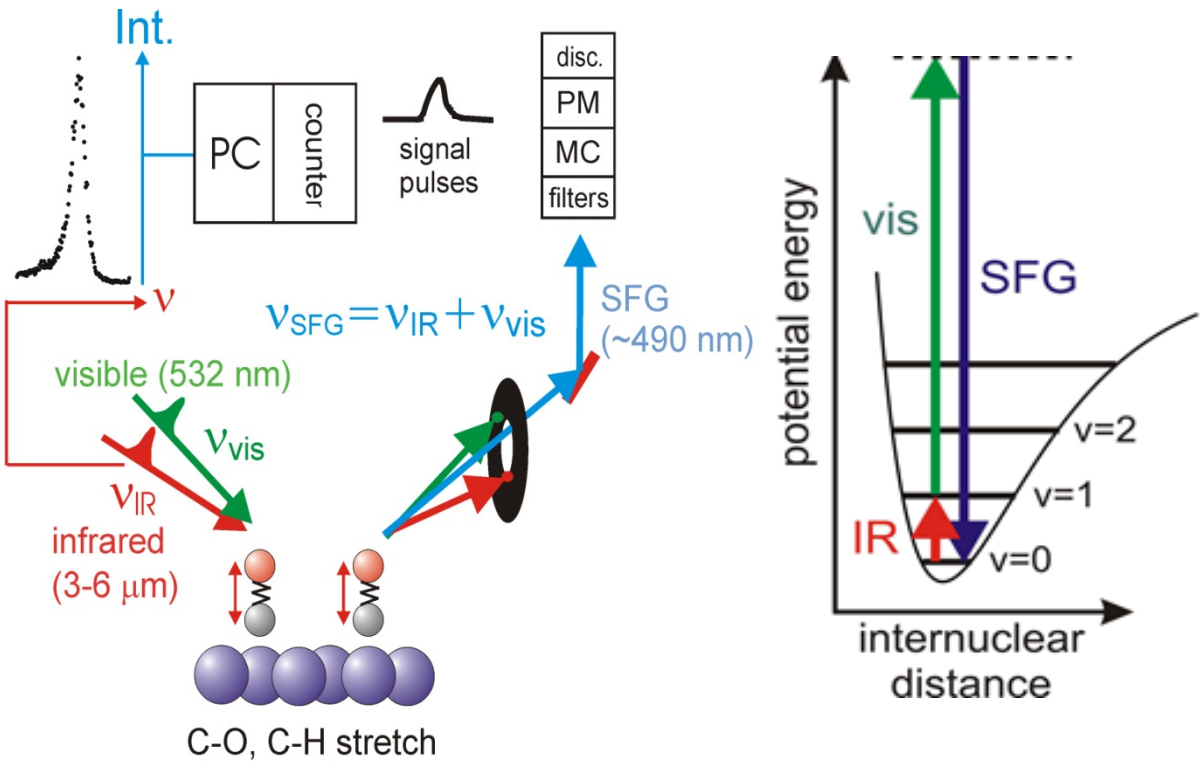

inherently surface sensitive (SFG not allowed in media with inversion symmetry due to 2nd order nonlinearity)

no signal from isotropic gas phase and centrosymmetric substrate → adsorbate spectra from UHV to 1 bar

IR-vis Sum Frequency Generation (SFG) Laser Spectroscopy: experimental

Laser spectroscopy (SFG)

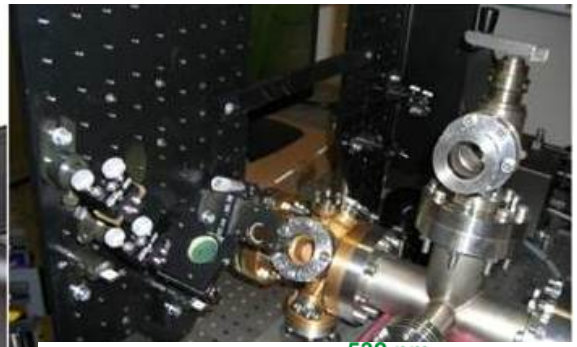

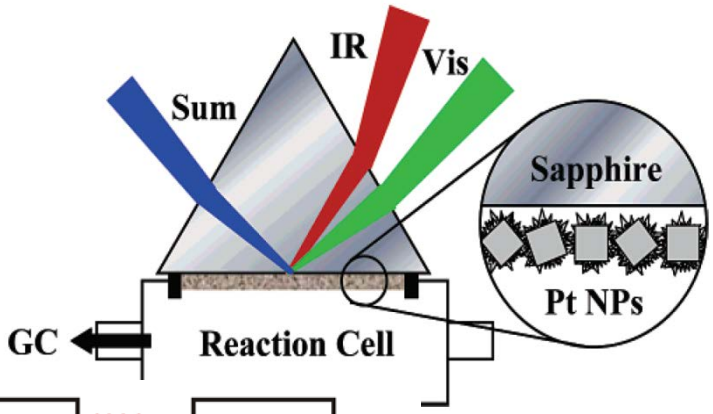

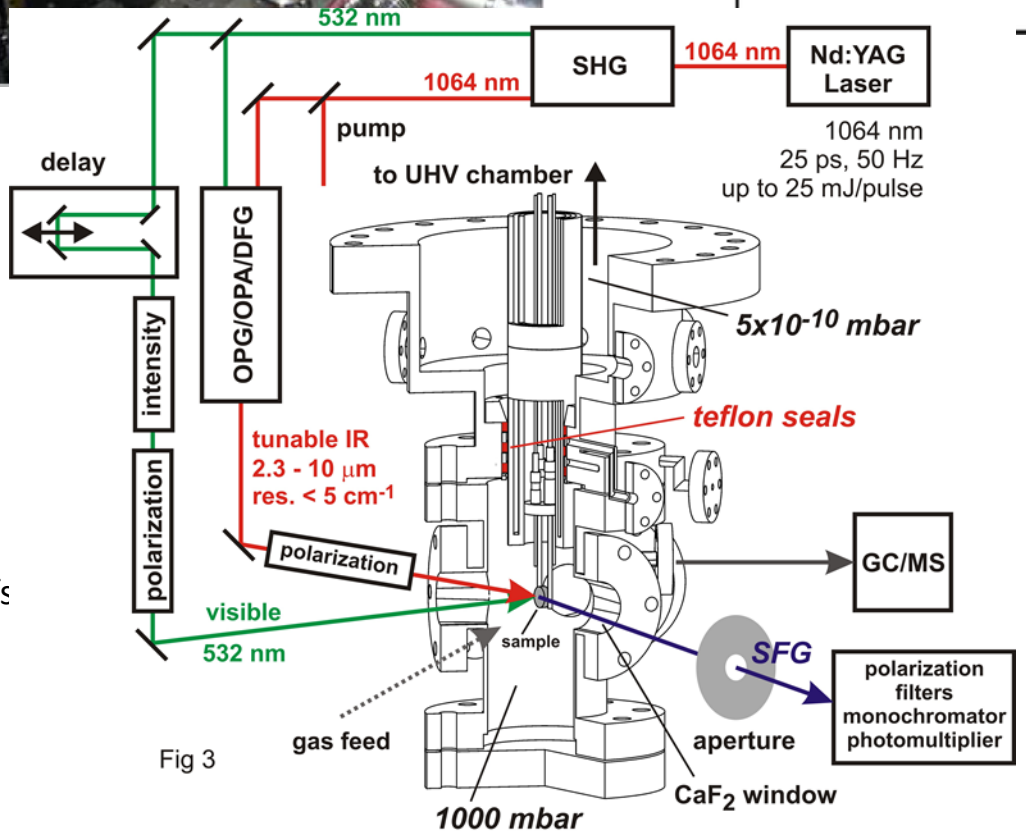

Fig 3

K. Föttinger et al., "Sum Frequency Generation and Infrared Reflection Absorption Spectroscopy“ in: "Characterization of Solid Materials and Heterogeneous Catalysts", Wiley-VCH, 2012. and refs therein

IR-vis Sum Frequency Generation (SFG) Laser Spectroscopy

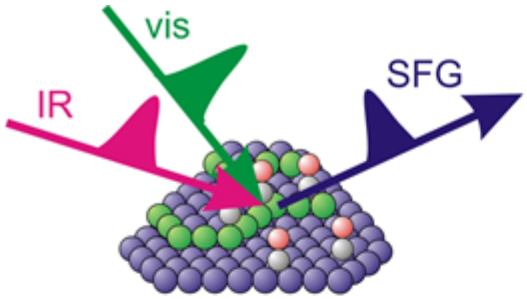

(a) scanning SFG

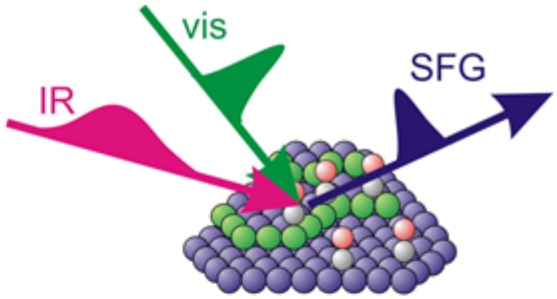

(b) broadband SFG

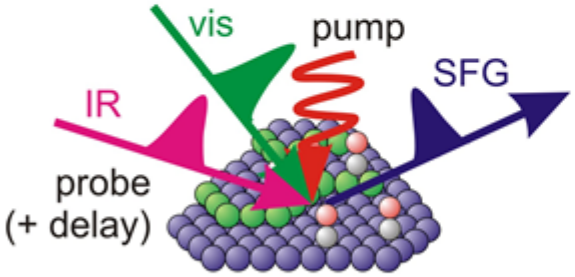

(c) time-resolved SFG

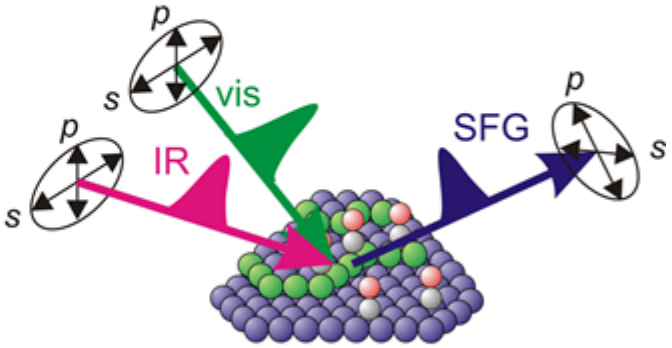

(d) polarization-dependent SFG

→ determine bond angles with respect to the surface / adsorption geometries

K. Föttinger et al., "Sum Frequency Generation and Infrared Reflection Absorption Spectroscopy“ in: "Characterization of Solid Materials and Heterogeneous Catalysts", Wiley-VCH, 2012. and refs therein

NAP-XPS

λ photoelectrons (PE):
10^5 Pa: 10^{-7} m
100 Pa: 10^{-4} m
10^{-8} Pa: 10^6 m

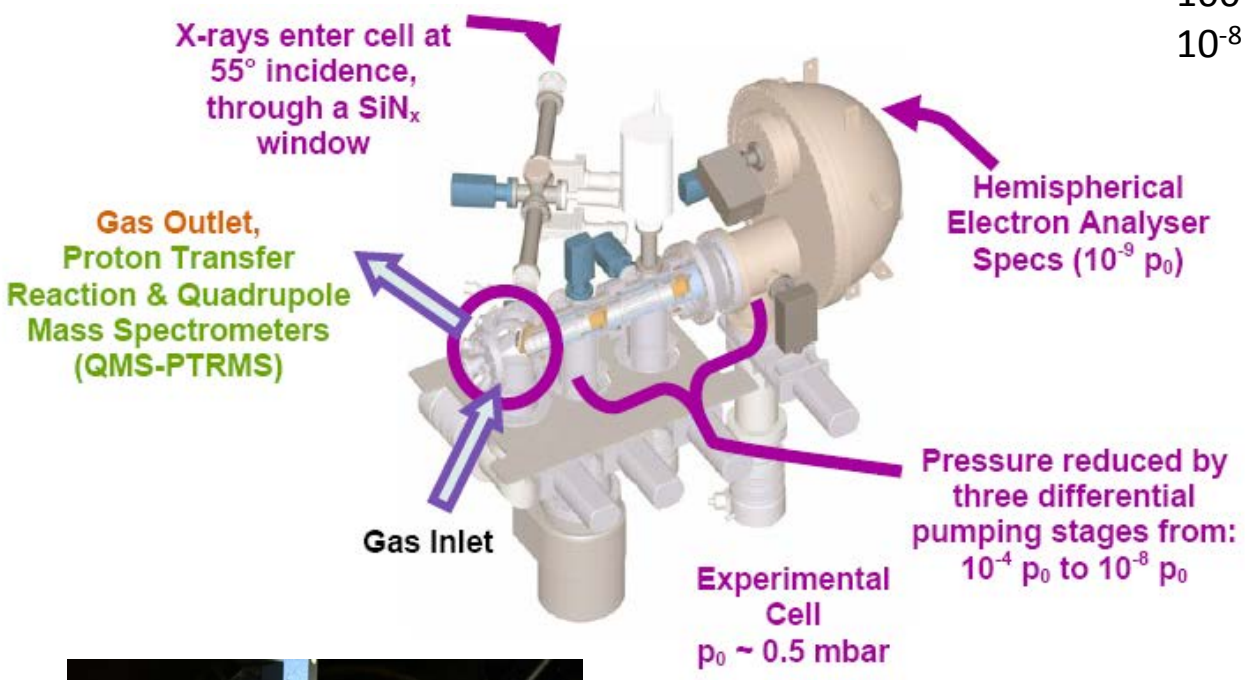

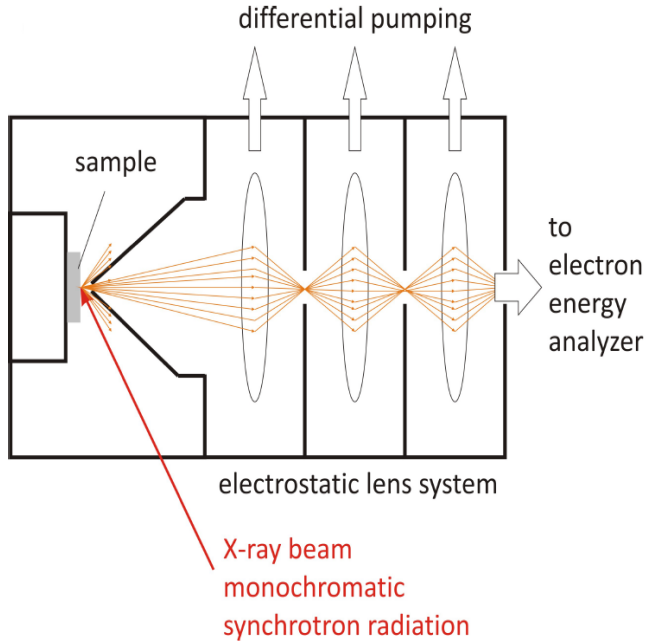

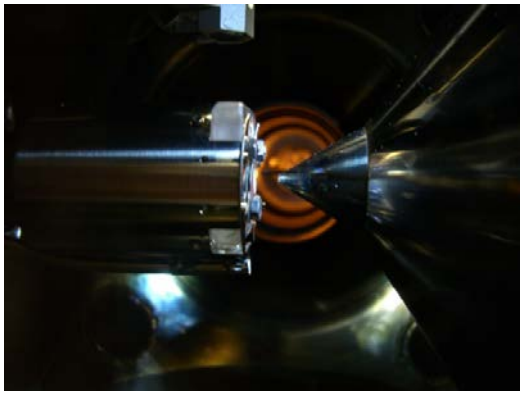

- up to mbar pressures
- differential pumping, short pathway of PE in gas atmosphere
- synchrotron radiation
- depth profiling by different $E_{h\nu}$
- flow cell connected to MS

ISISS Beamline U49/2-PGM1 at BESSY, http://www.fhi-berlin.mpg.de

NAP-XPS

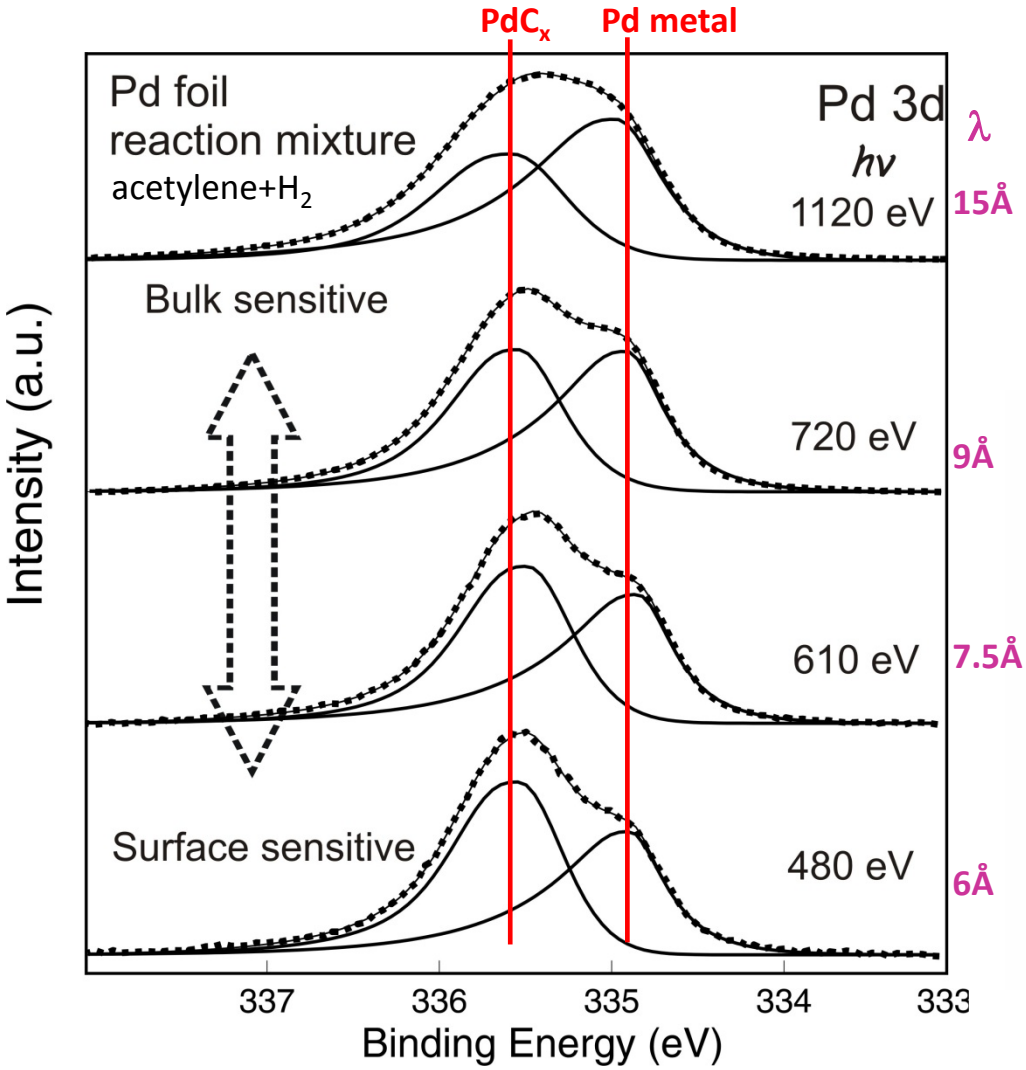

Variation of photon energy
→ different E_{kin}(PE)

$$E_b = h\nu - E_{kin} - \varphi$$

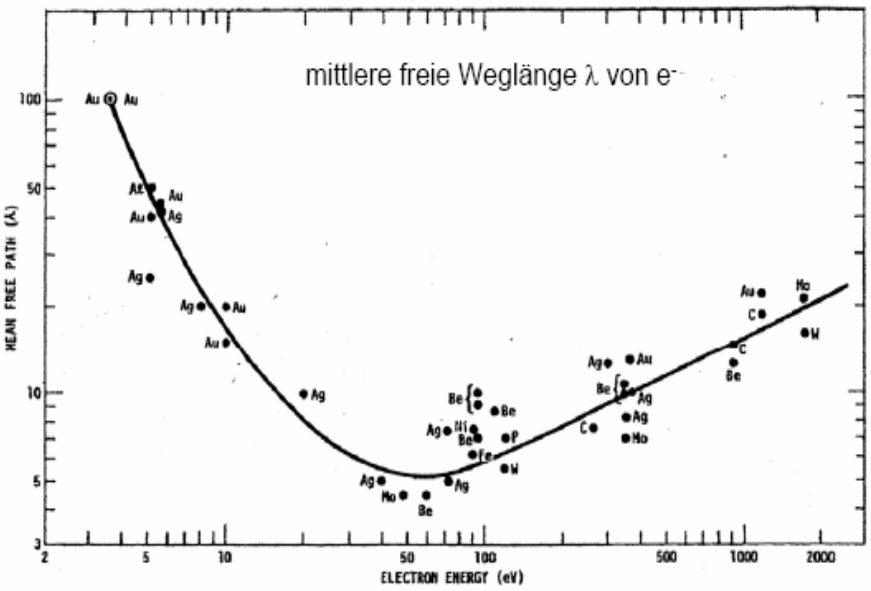

ISISS Beamline U49/2-PGM1 at BESSY, http://www.fhi-berlin.mpg.de
D. Teschner et al.

4. Case studies and examples

4.1 Vibrational Spectroscopy of CO on metal surfaces: band assignment

strong dynamic dipole -> strong signal
C-O stretch frequency -> binding site

CO frequency = f (metal, structure, CO coverage)

on-top	bridge-bonded	3-fold hollow
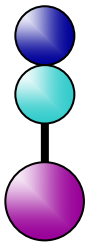	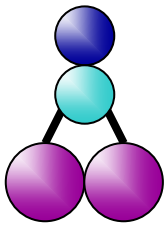	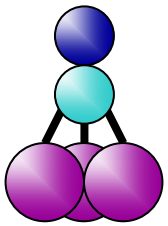
2000 – 2130	1880 – 2000	1800 – 1880

(cm^{-1})

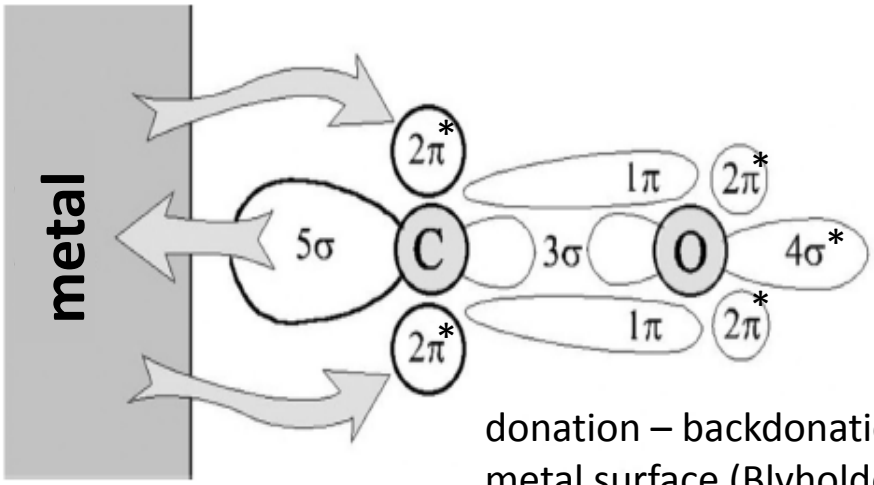

donation – backdonation model for CO bonding to metal surface (Blyholder model)

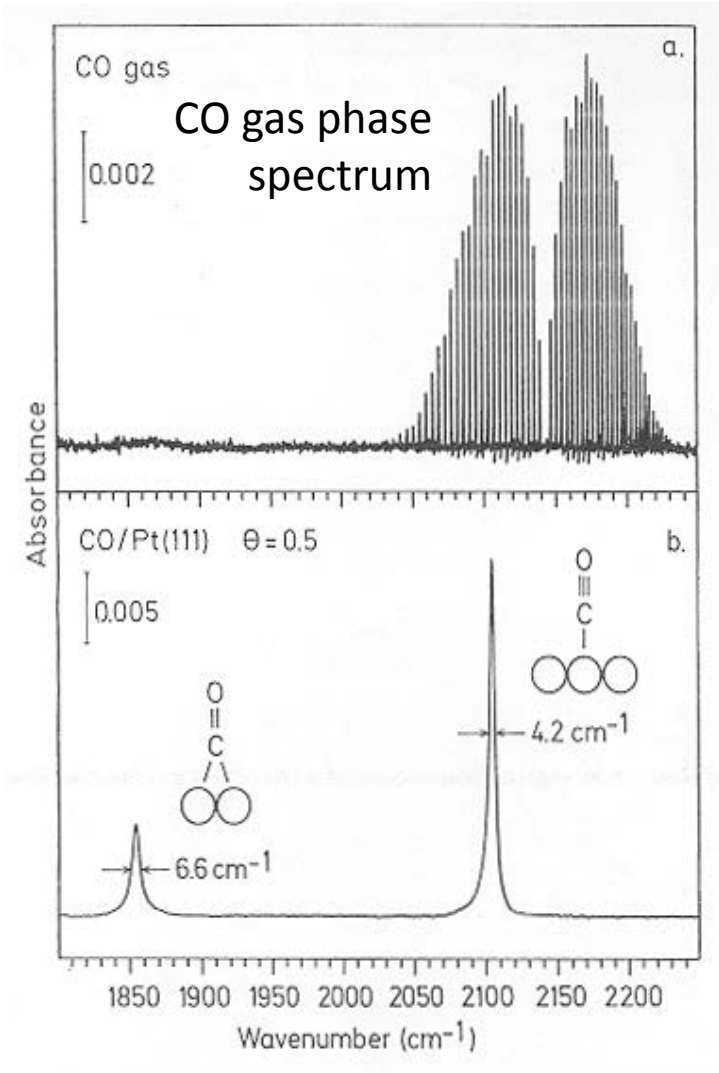

CO on Pt(111) 10^{-7} mbar

CO structures on Pd(111) under UHV: combining LEED and PMIRAS for band assignment

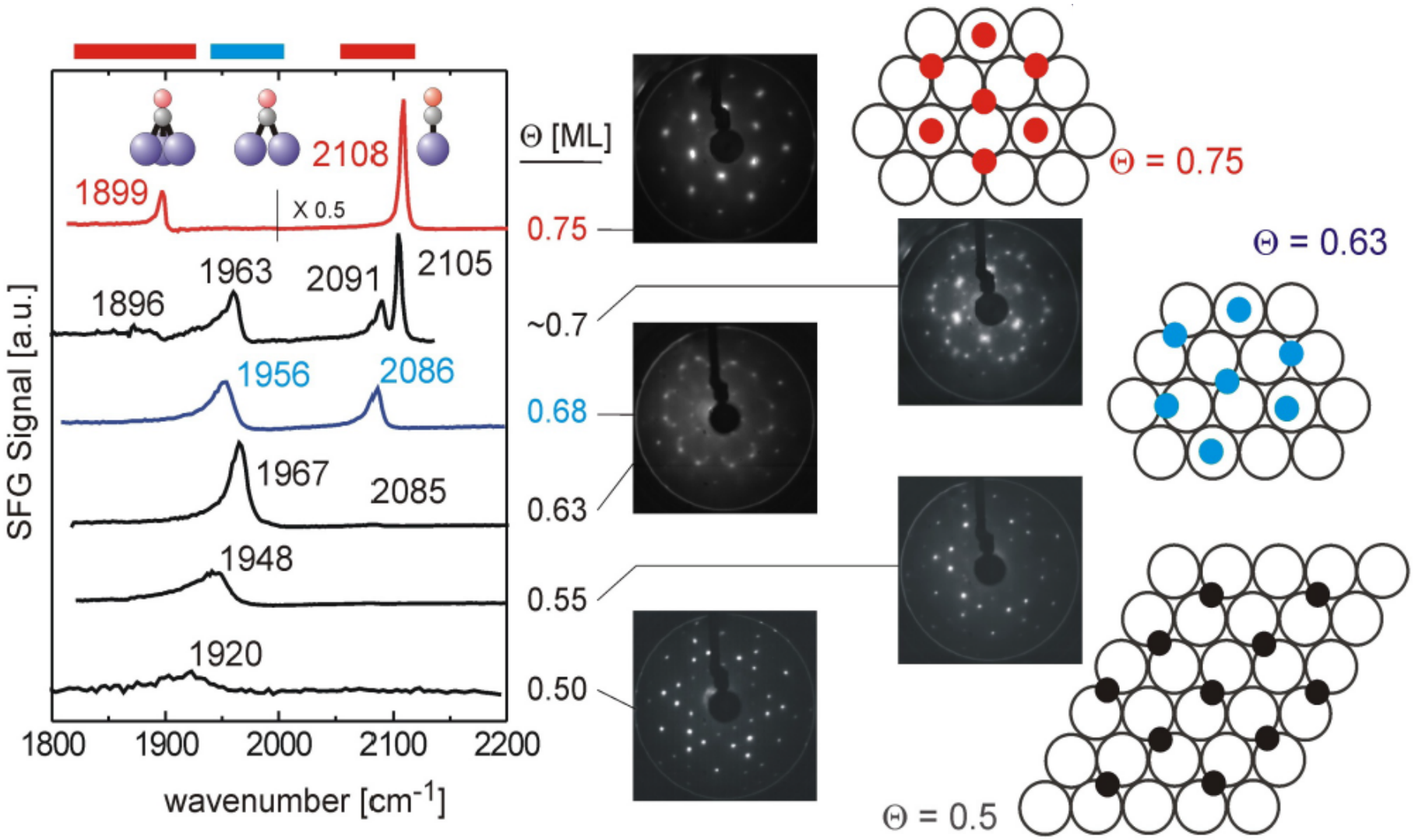

G. Rupprechter, Phys.Chem.Chem.Phys. 3 (2001) 4621. H. Unterhalt et al., J. Phys. Chem. B 106 (2002) 356.

4.2 PdZn intermetallic compounds (IMC) in methanol steam reforming (MSR)

- methanol steam reforming (MSR):

  source of hydrogen: $CH_3OH + H_2O \rightarrow CO_2 + 3H_2$

- challenge: no CO (poison e.g. for fuel cells)

  by methanol decomposition

  $CH_3OH \rightarrow CO + 2H_2$

- commercial catalyst: Cu/ZnO

  active and selective, low stability

- Pd on inert supports completely unselective,

  but Pd/ZnO and Pd/Ga_2O_3 promising

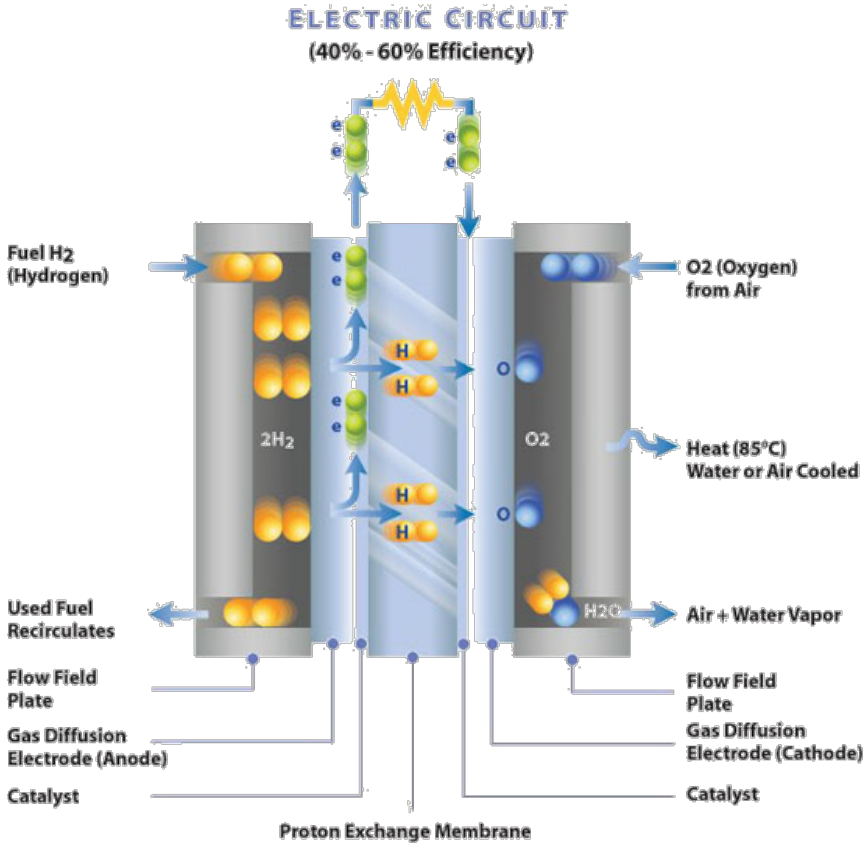

source: www.ballard.com

Catalytic properties of powder catalysts:

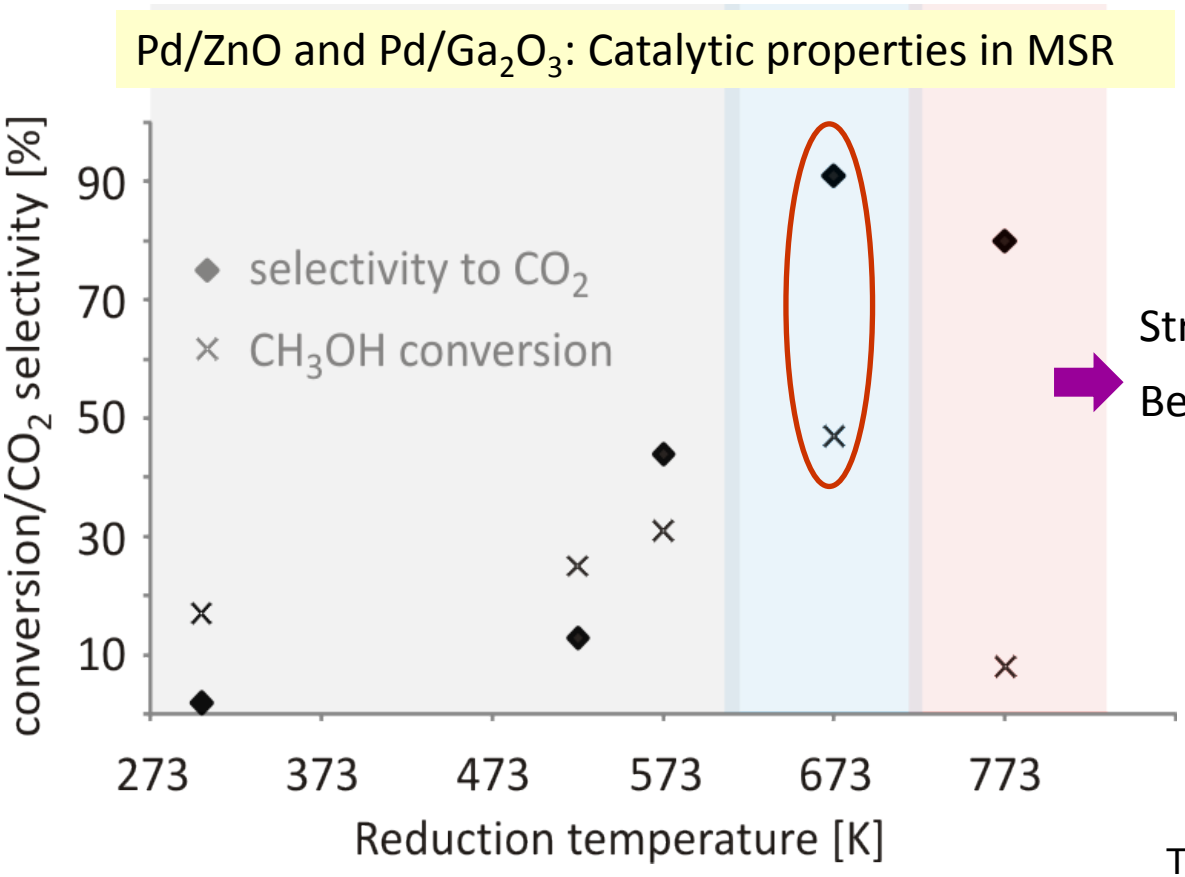

Strong influence of T_{red}

Best catalytic performance after reduction at 673 K

Fixed-bed flow reactor,
$T_{reaction}$=523 K; p_{MeOH}=p_{H2O}=40 mbar

totally different catalytic performance than Pd metal → formation of $PdZn/Pd_xGa_y$ IMC upon reduction

A. Haghofer, K. Föttinger, F. Girgsdies, D. Teschner, A. Knop-Gericke, R. Schlögl, G. Rupprechter, J. Catal. 286 (2012) 13.

Structural properties of powder catalysts:

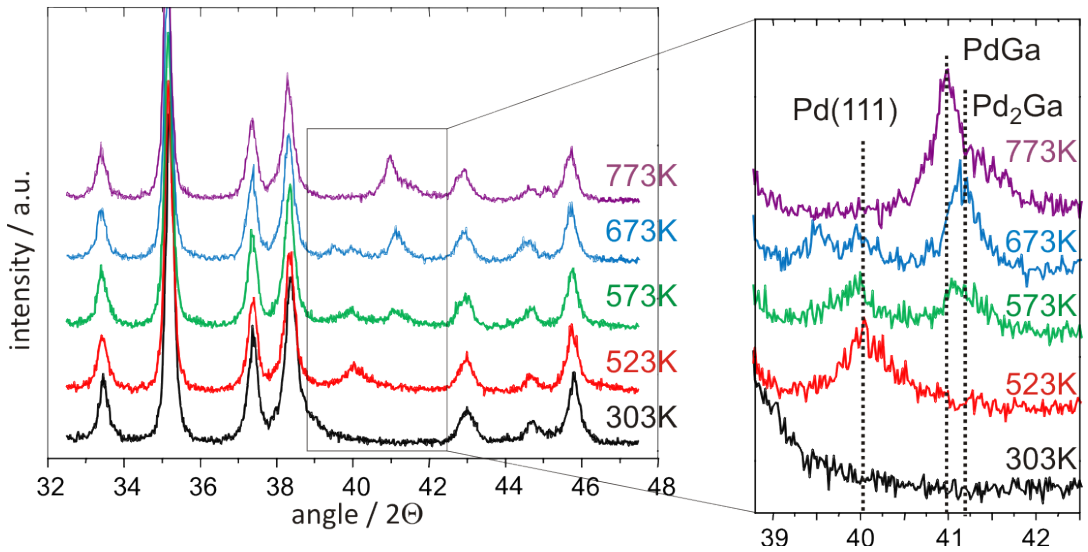

In situ XRD – stepwise temperature increase in 25% H_2/He

increasing T in H_2

- $PdGa / Ga_2O_3$
- Pd_2Ga / Ga_2O_3
- $Pd+Pd_2Ga / Ga_2O_3$
- Pd / Ga_2O_3
- $Pd(H) / Ga_2O_3$

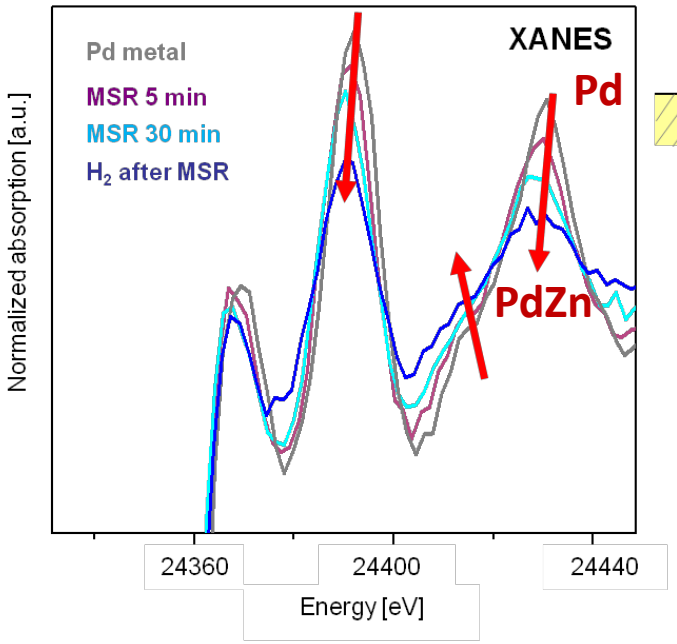

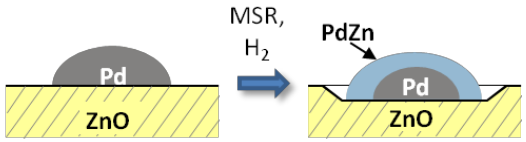

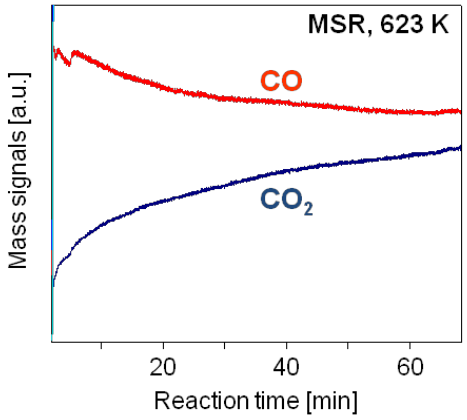

In situ XAS – during reaction at 623 K

A. Haghofer, K. Föttinger, et al., J. Catal. 286 (2012) 13.

K. Föttinger, J.A. van Bokhoven et al., J. Phys. Chem. Lett. 2 (2011) 428.

K. Föttinger, G. Rupprechter, Acc. Chem. Res. 47 (2014) 3071.

Possible explanations for different reactivity of PdZn

activation barrier for MeOH dehydrogenation

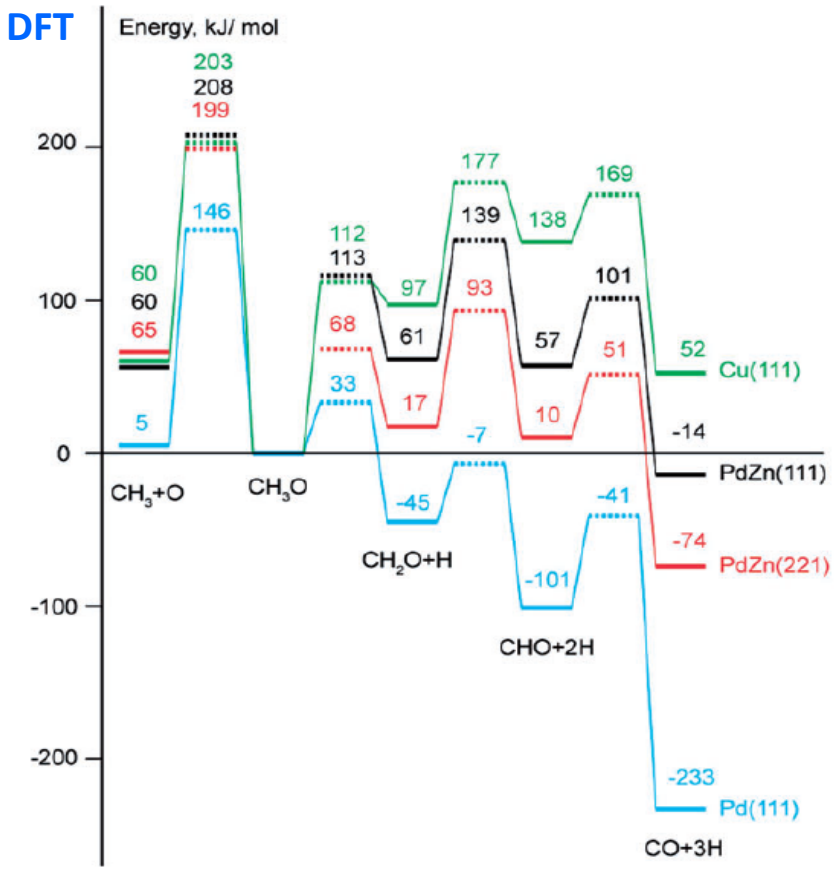

valence band spectra

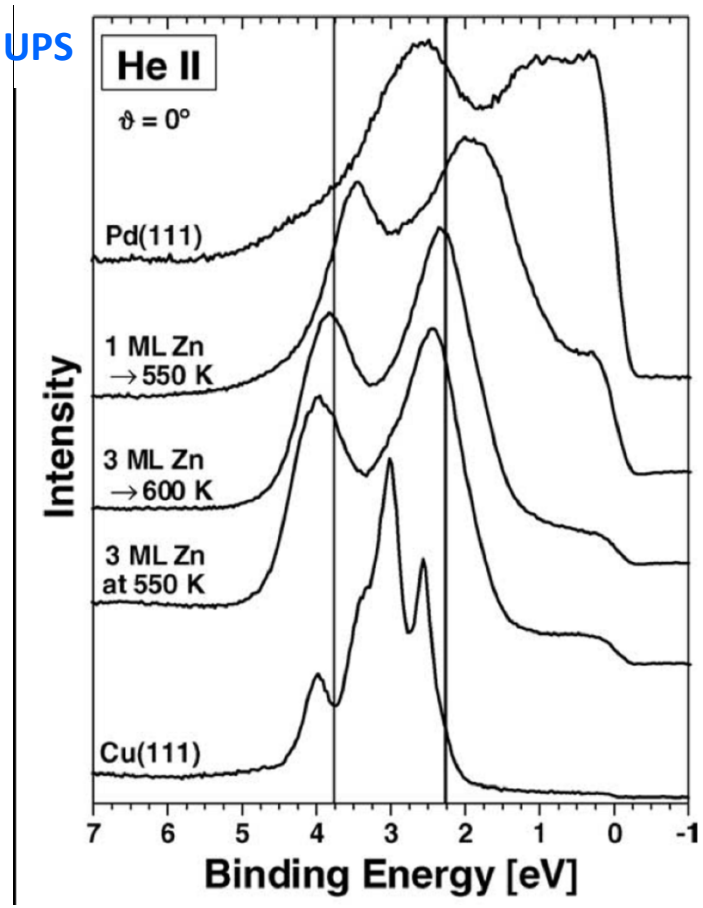

electronic properties of PdZn similar to Cu

K.M. Neyman et al., *PCCP*, **2007**, *9*, 3470

A. Bayer, et al., *Surf. Sci.*, 2006, **600**, 78

Preparation of PdZn surface alloy as model system

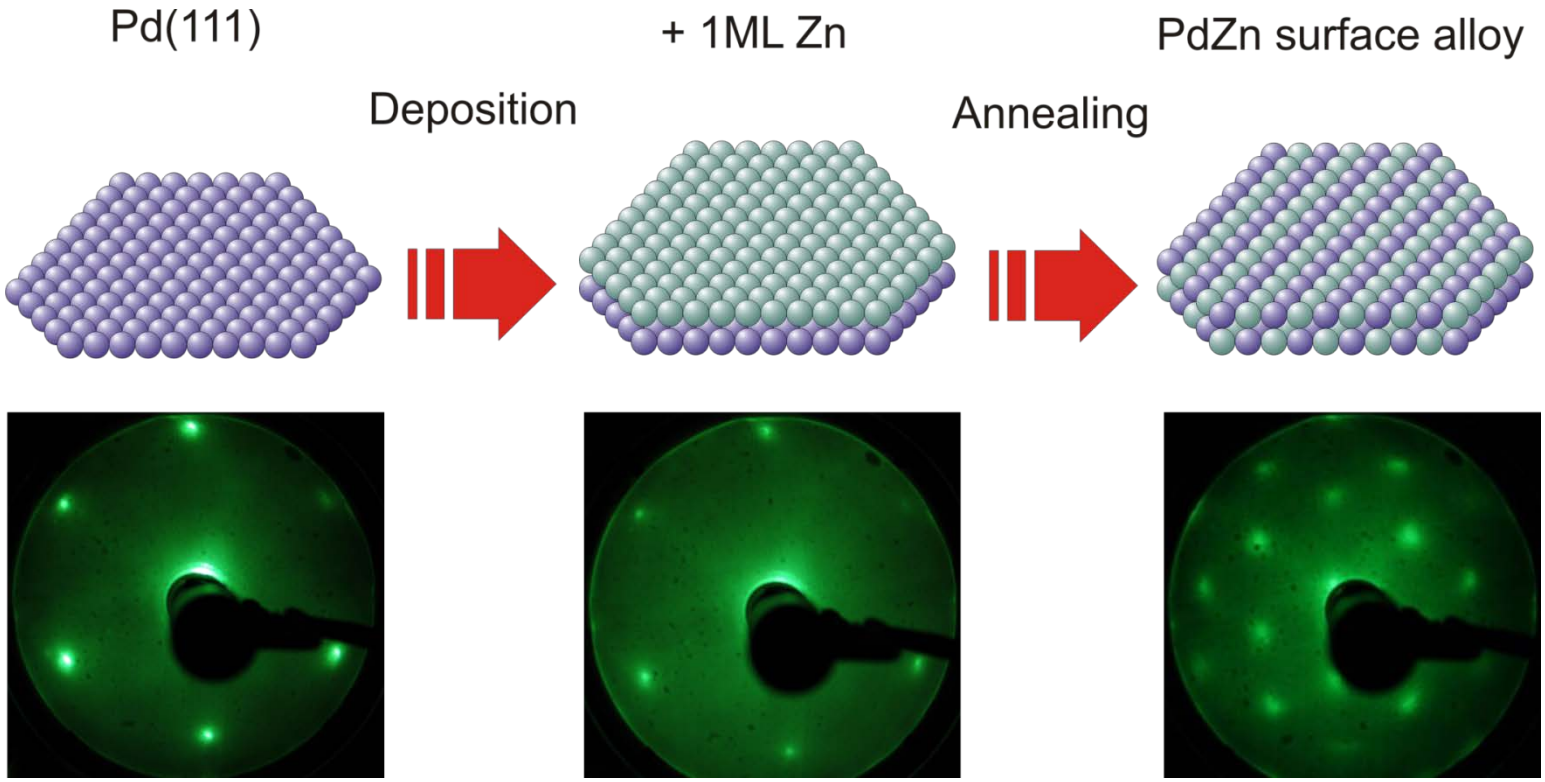

- evaporation of Zn (0.5 – 3 ML) at l-N_2 temperature or 300 K
- annealing (3 min) at 550 K
- formation of 1:1 Pd:Zn surface alloy
- 2x1 surface periodicity

A. Bayer, et al., *Surf. Sci.*, 2006, 600, 78.
C. Weilach, S. Kozlov, H. Holzapfel, K. Föttinger, K M Neyman, G. Rupprechter, J. Phys. Chem. C, 116 (2012) 18768.
Weirum, G., Bako, I., Winker, A., Surnev, S., Netzer, F.P., Schennach, R. et al., J. Phys. Chem. C, 2009, 113, 8788

Preparation of PdZn surface alloy: XPS

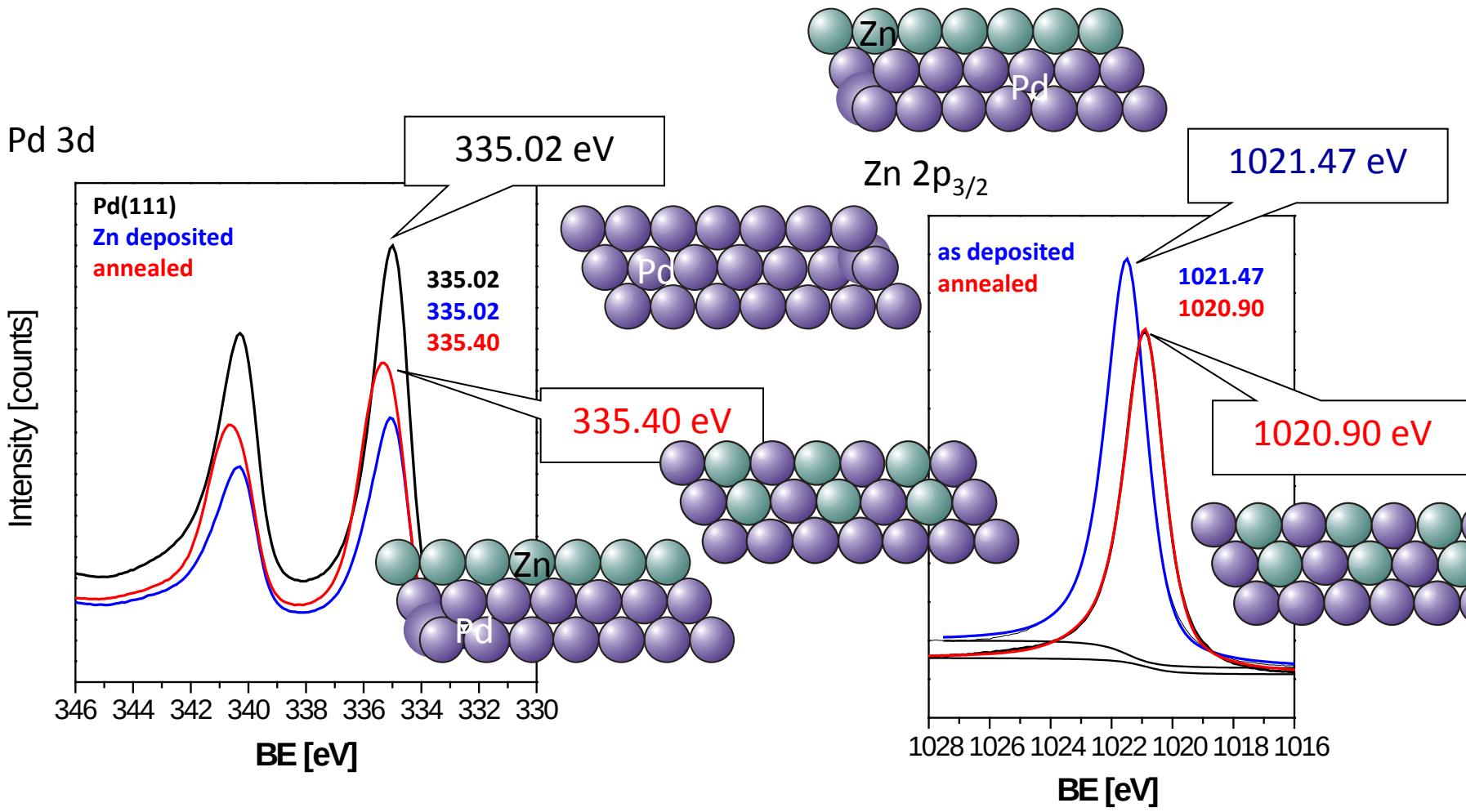

deposition of 1 ML Zn on Pd substrate

intermixing and alloy formation upon annealing

Bayer A et al., *Surface Science*, **2006**, *600*, 78
Weilach C., PhD thesis

Comparison vibrational spectroscopy of CO adsorption on PdZn/ZnO powder catalyst and PdZn surface alloy model system: excellent agreement

Characteristic band at 2070 cm^{-1} at saturation coverage (i.e. 0.5 ML from TPD)

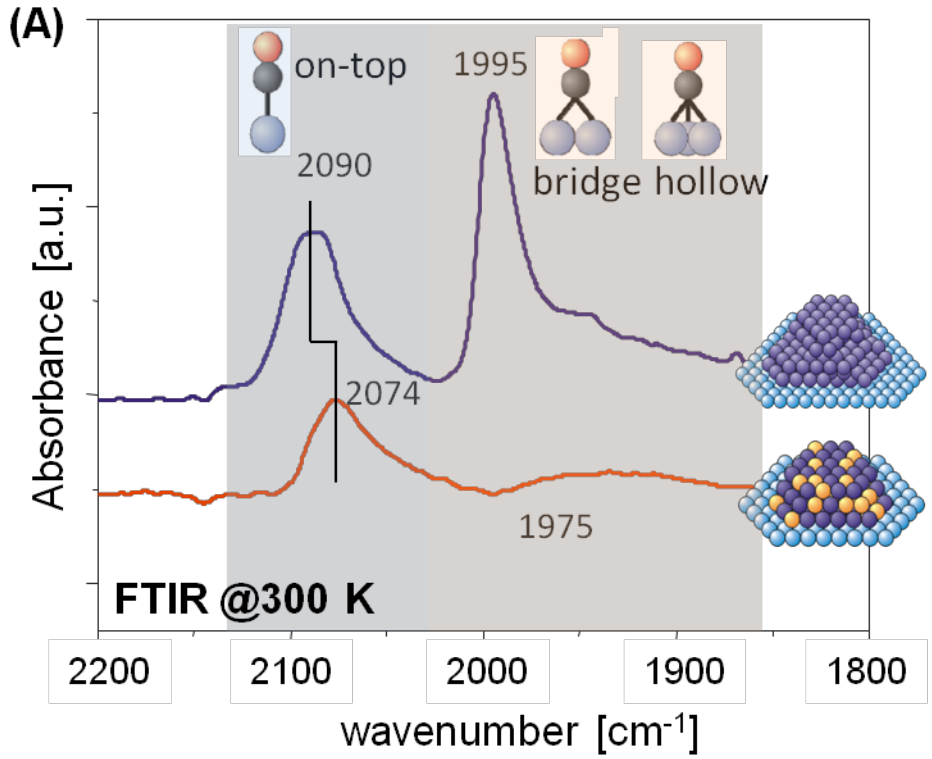

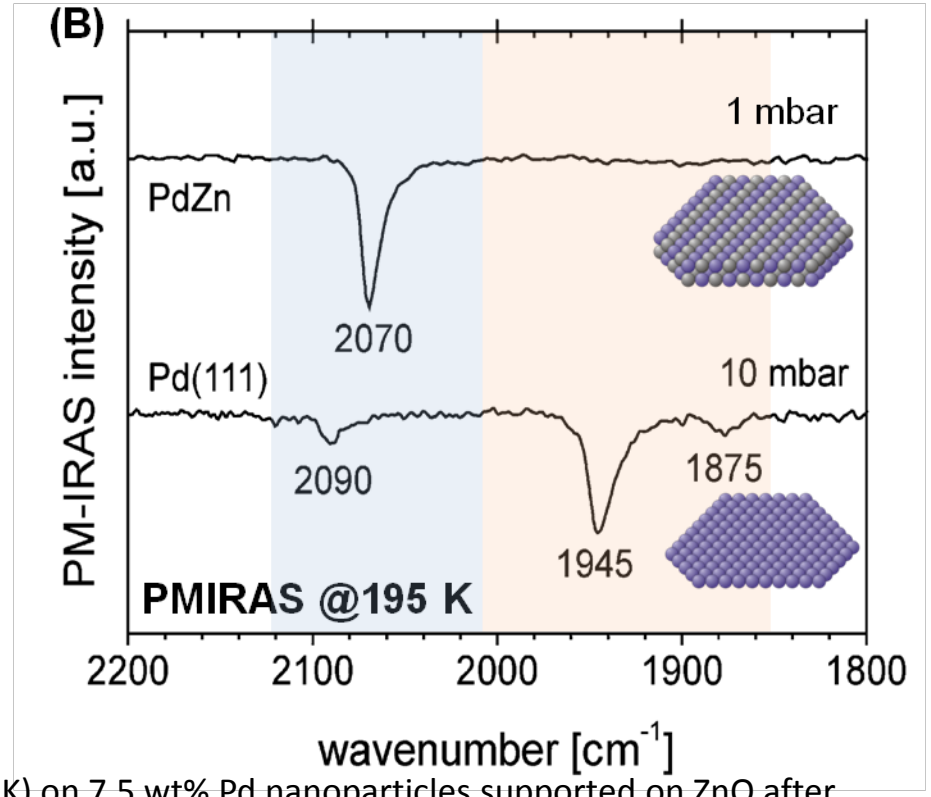

(A) Transmission FTIR spectra of CO adsorption (5 mbar, 303 K) on 7.5 wt% Pd nanoparticles supported on ZnO after reduction at 303 K (upper spectrum, representing Pd/ZnO) and 623 K (lower spectrum, representing PdZn/ZnO). (B) PMIRAS spectra of CO adsorption at 195 K on a 4 ML PdZn/Pd(111) model catalyst annealed to 550 K and on Pd(111).

K. Föttinger, J.A. van Bokhoven, M. Nachtegaal, G. Rupprechter, J. Phys. Chem. Lett. 2 (2011) 428.

C. Weilach, S. Kozlov, H. Holzapfel, K. Föttinger, K M Neyman, G. Rupprechter, J. Phys. Chem. C, 116 (2012) 18768.

NAP-XPS of PdZn surface alloy : new insights

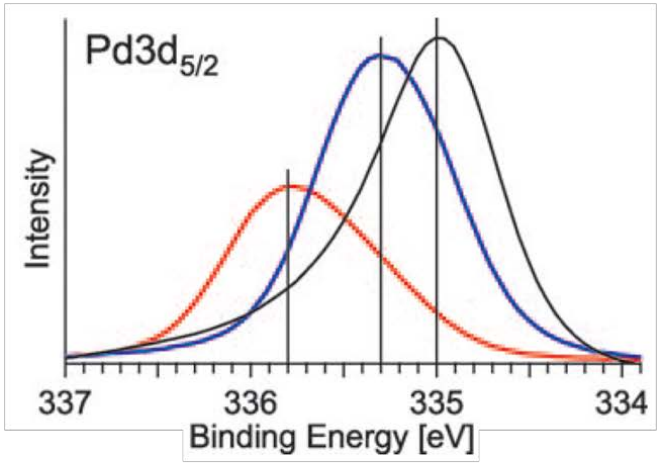

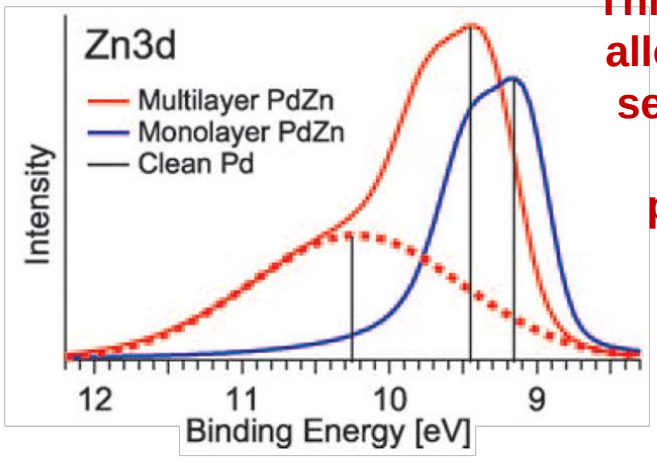

Thickness of the alloy matters → selectivity and electronic properties !

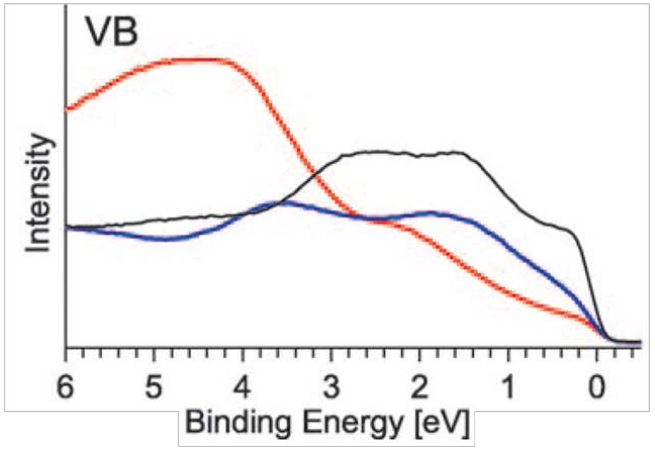

NAP-XPS spectra (Pd 3d, Zn3d, and valence-band (VB) regions; BESSY II) acquired in situ during MSR on the PdZn 1:1 multilayer (red traces) and monolayer alloy (blue traces). For comparison, the corresponding "pure" Pd spectra are added (black traces). The oxidized ZnOH component is highlighted by the dotted red line (middle panel). To obtain equal information depth for all spectra the Pd3d spectra were recorded with 650 eV photon energy, the Zn3d and valence-band regions at 120 eV. Reaction conditions: 0.12 mbar methanol, 0.24 mbar water, 553 K.

C. Rameshan et al., Angew. Chem. Int. Ed. 49 (2010) 3224.

Low-energy ion scattering spectroscopy (LEIS)

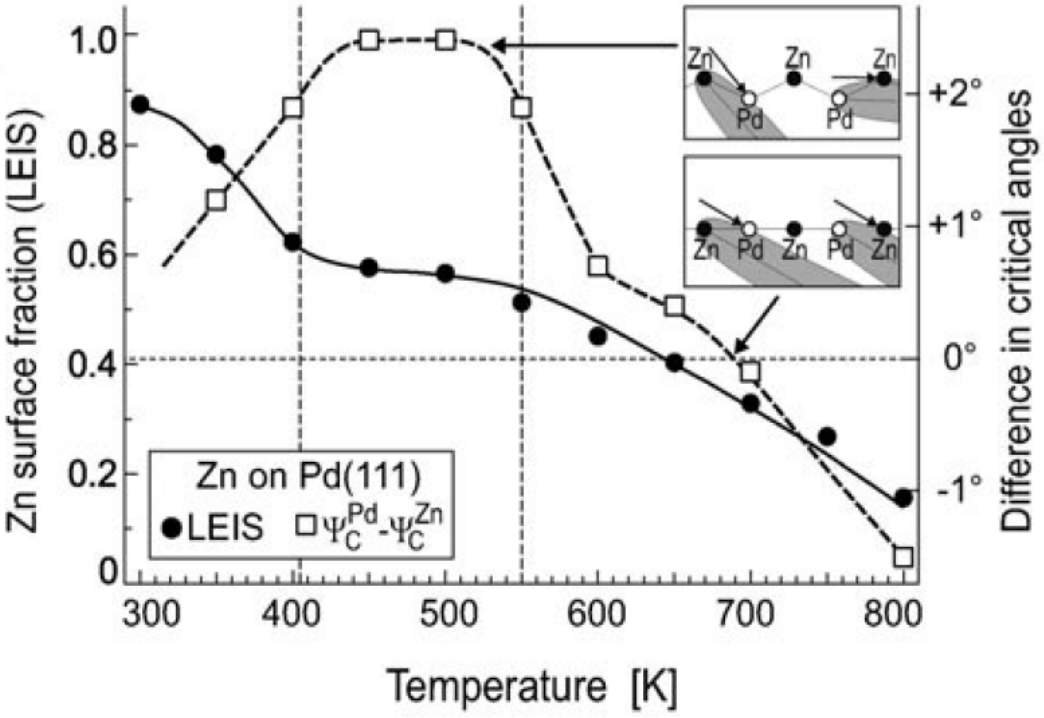

Corrugation changes with thickness of the alloy

● Pd:Zn surface fractions derived from LEIS for Zn films deposited on Pd(111). ○ Difference in critical angles for backscattering of 5 keV Ne ions from Pd and Zn atoms. Inset: schematic side views of a corrugated and a non-corrugated (2x1) PdZn surface. Arrows and gray shadow cones indicate the critical angles where backscattering from Pd and Zn atoms, respectively, sets in.

C. Rameshan et al., Angew. Chem. Int. Ed. 49 (2010) 3224.

4.3 Carbonate formation on alumina surfaces

γ-Al_2O_3 powder catalyst:

Vibrational IR spectra after adsorption of CO and CO_2 (5 mbar, 293 K) on Pd-Al_2O_3 and Al_2O_3: (A) carbonate region and (B) OH stretching region

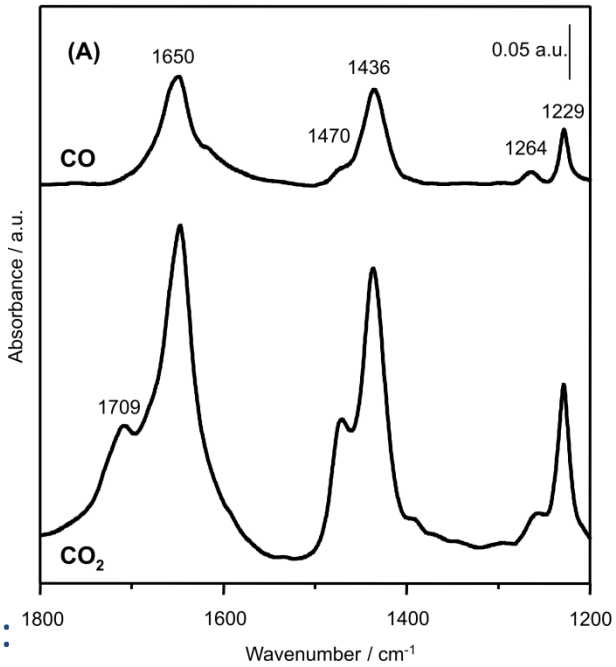

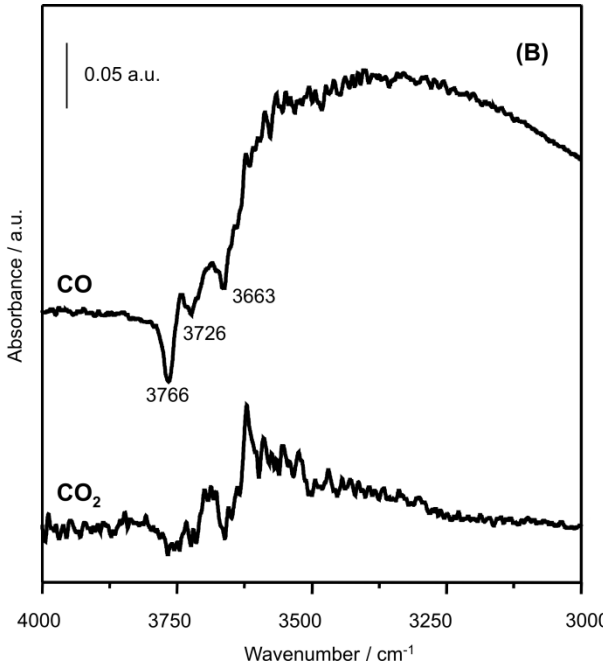

Proposed reaction mechanism:

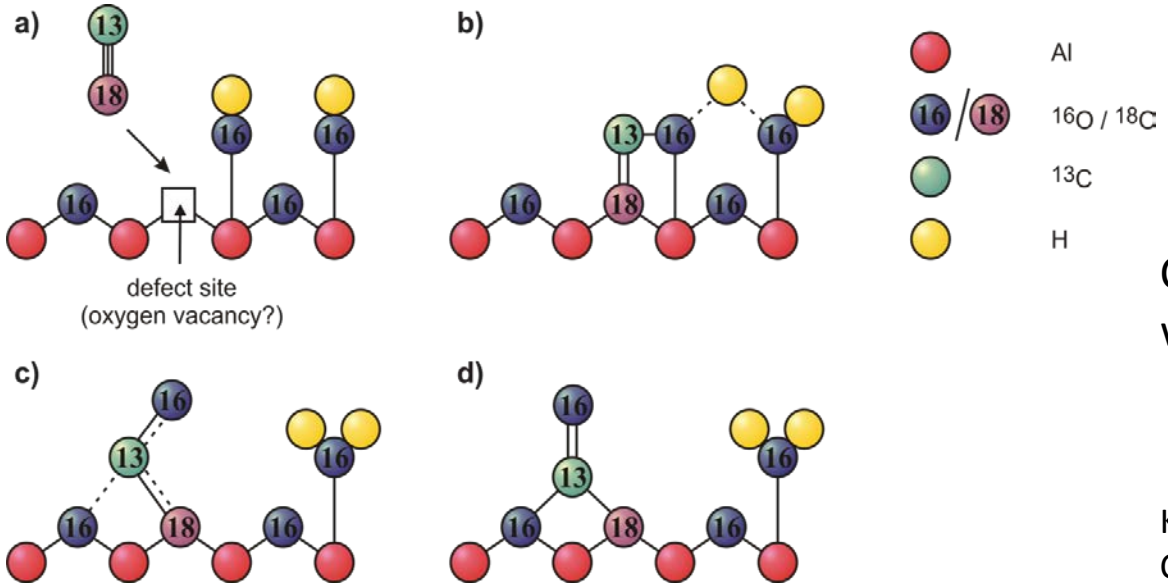

Carbonate formation from CO: water-gas shift type reaction

$$CO + OH \rightarrow CO_2 + \tfrac{1}{2} H_2$$

K. Föttinger, R. Schlögl, G. Rupprechter, Chem. Commun. (2008), 320 .

Al_2O_3 thin film on NiAl (110) as model catalyst

Preparation:

- NiAl(110) single crystal surface
- cleaned by sputtering in 1x10^{-5} mbar argon (1 kV ion energy) at 800 K for 60 min, followed by annealing in vacuum for 5 min at 1150 K to heal the surface structure.
- oxidation at 550 K for 15 minutes in 1x10^{-6} mbar O_2, followed by annealing in vacuum at 1100 K for 3 minutes. oxidation/annealing repeated twice to obtain well-ordered alumina films
- contrary to high surface area alumina, the model system of Al_2O_3/NiAl(110) exhibits few defect sites and is intrinsically free of hydroxyl groups
- defect-enriched films were prepared by additionally sputtering the as-prepared alumina film at reduced pressure (1x10^{-6} mbar Ar) up to 5 min.

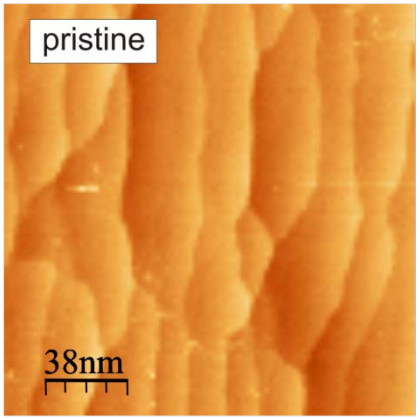

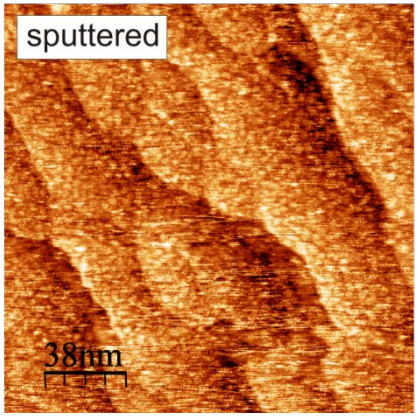

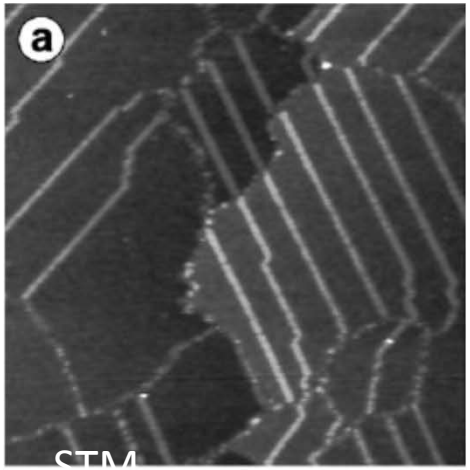

Al_2O_3 trilayer

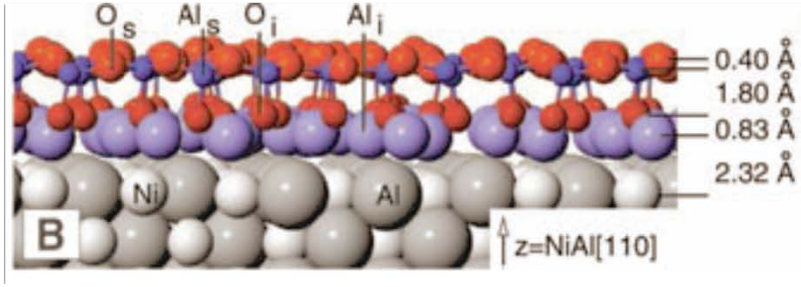

C. Weilach, C. Spiel, K. Föttinger, G. Rupprechter, Surface Science, 605 (2011), 1503

Al_2O_3 thin film model catalyst

Carbonate formation from CO and CO_2: XPS and PMIRAS

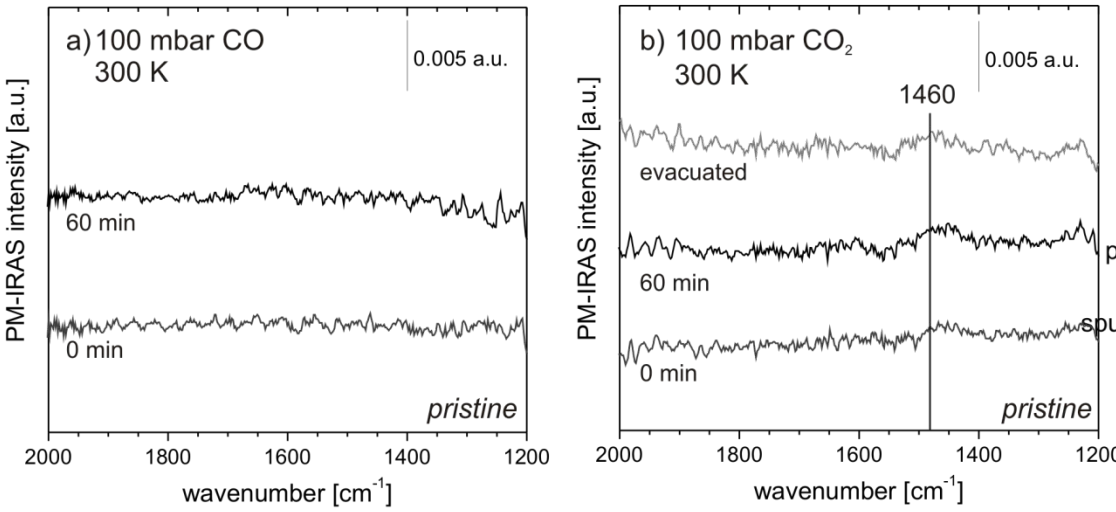

PM-IRAS surface spectra of the pristine Al_2O_3/NiAl(110) film acquired in 100 mbar CO (a) and 100 mbar CO_2 (b). The topmost trace in b) was taken after CO_2 was removed from the HP-cell.

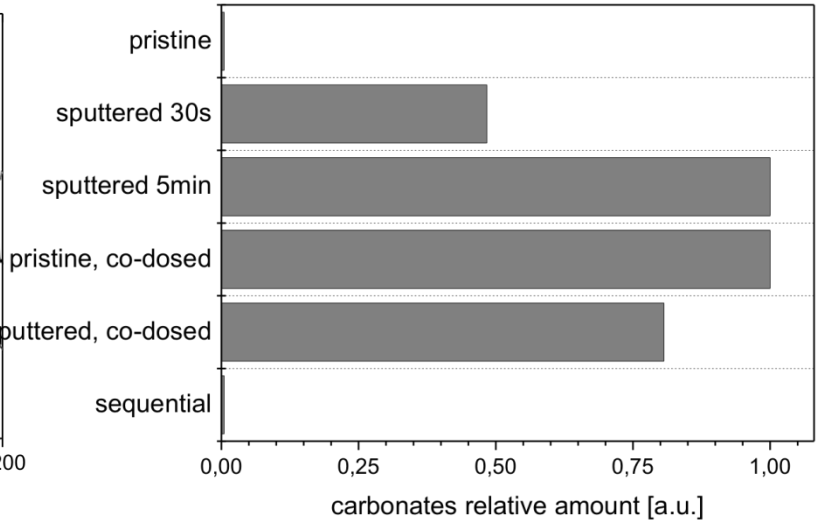

Relative amount of carbonates upon mbar CO_2 exposure as derived from XPS C 1s peak areas. The area of the carbonate signal for the 5 min sputtered film was taken as reference (1).

- no carbonates under UHV conditions
- monodentate carbonates in a 100 mbar CO_2 : IR band at 1460 cm^{-1}, peak in XPS C 1s region at 291 eV
- surface concentration of carbonates increased after generating defects by Ar^+ ion bombardment: reaction of coordinatively unsaturated O^{2-} ions of alumina with CO_2
- **no carbonates detected from CO even upon mbar CO exposure due to the absence of the required OH-groups (in agreement with the "water gas shift" mechanism)**

C. Weilach, C. Spiel, K. Föttinger, G. Rupprechter, Surface Science, 605 (2011), 1503

4.4 Methanol oxidation on Pd(111) and Pd nanoparticles on Al_2O_3/NiAl(110)

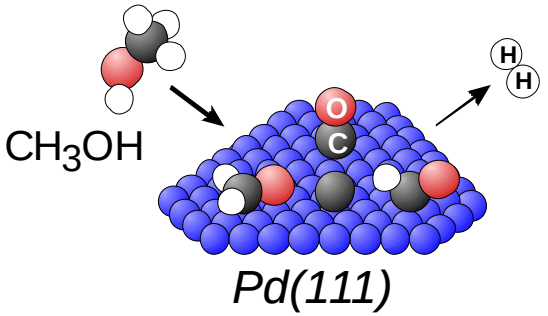

Reaction pathways on a metal surface:
Methanol decomposition and oxidation

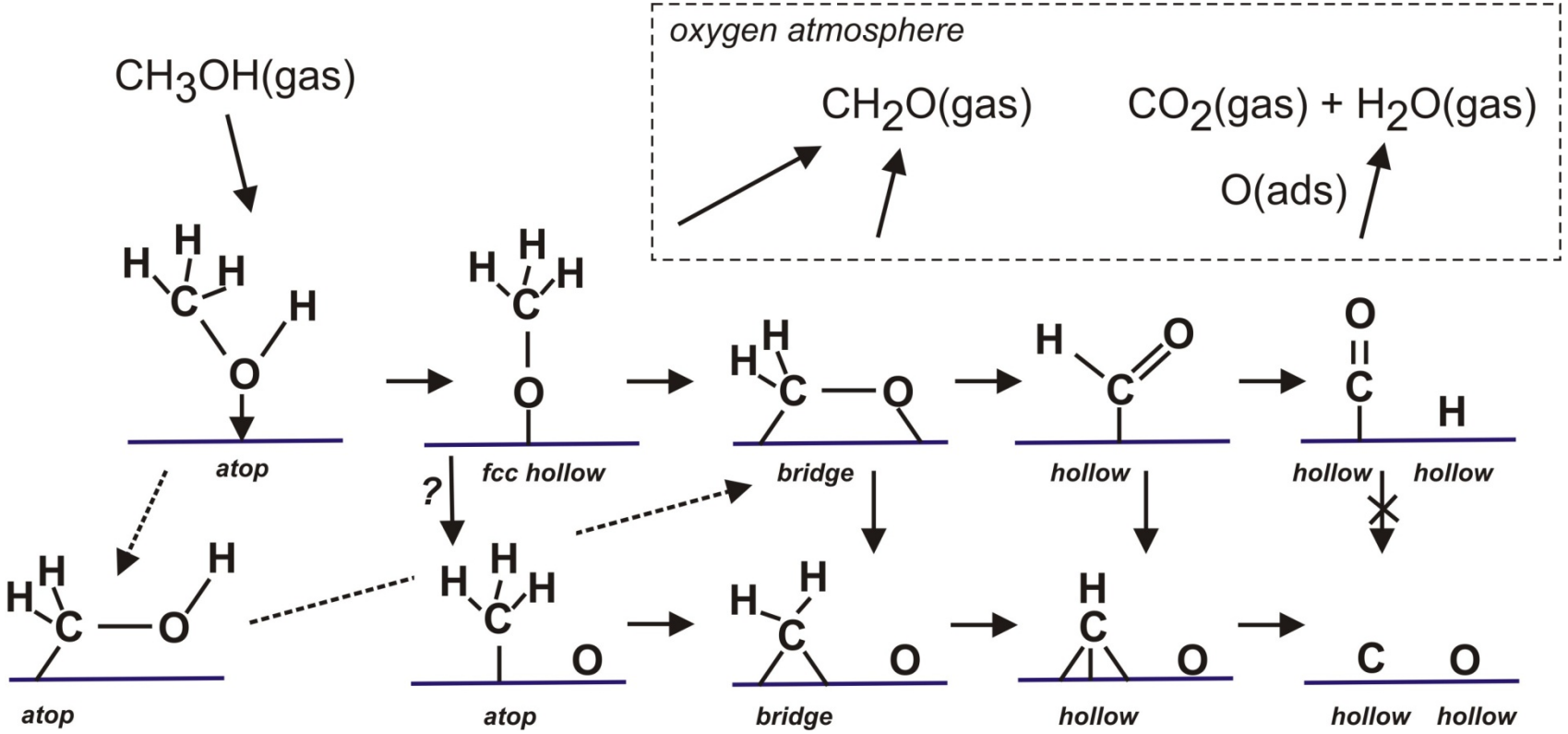

Methanol decomposition on Pd(111)

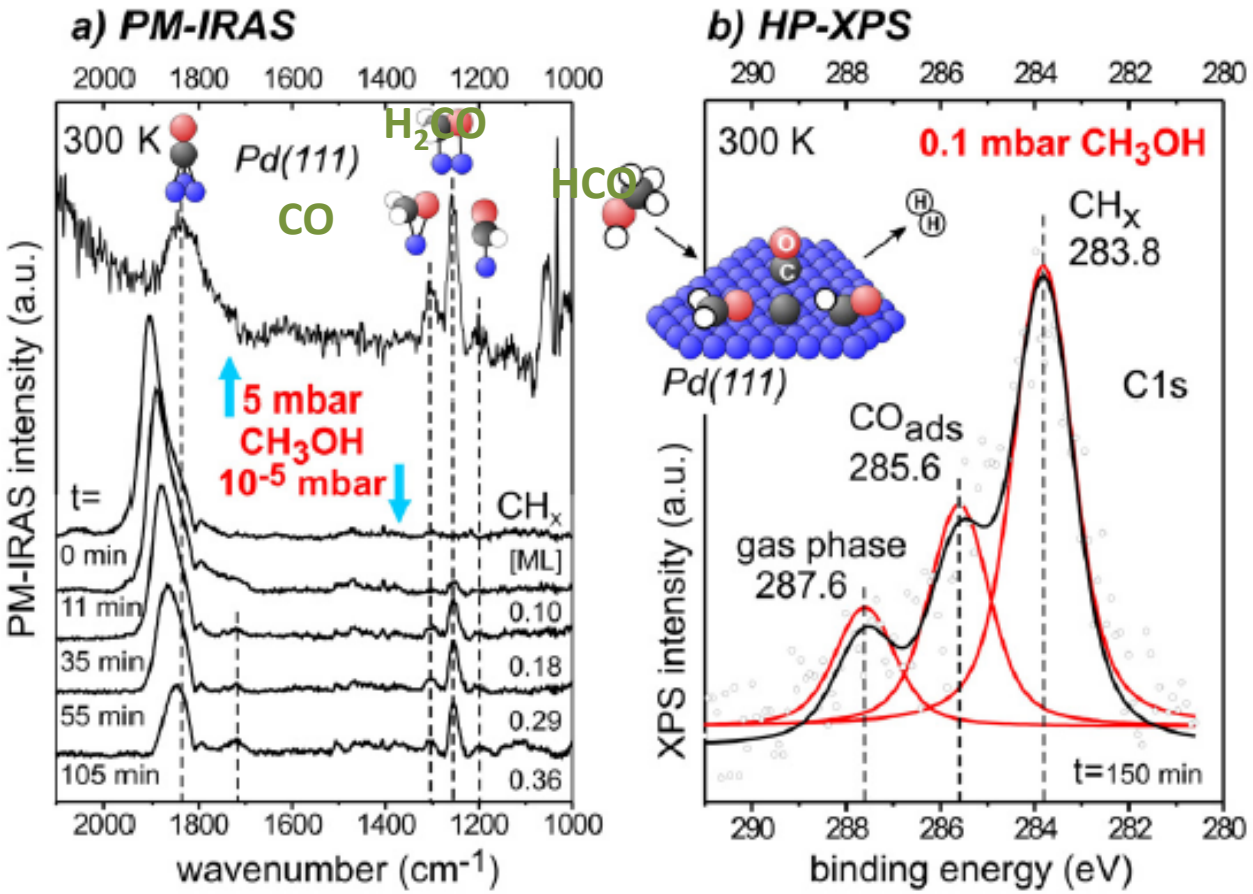

Detected surface species:
dehydrogenation pathway
and
C-O bond scission pathway

Figure 5. (a) PM-IRAS (p – s) surface vibrational spectra and (b) HP-XPS spectrum measured during CH_3OH decomposition on Pd(111) at 300 K, with the various species indicated. The time-dependent evolution of CH_2O (as observed by PM-IRAS) and of CH_x (values deduced from XPS) upon methanol decomposition at $\sim 10^{-5}$ mbar in (a) suggests a correlation between the two species. Adapted in part from [32]

G. Rupprechter, C. Weilach, J. Phys.: Condens. Matter 20 (2008) 184019

Methanol decomposition on Pd(111)

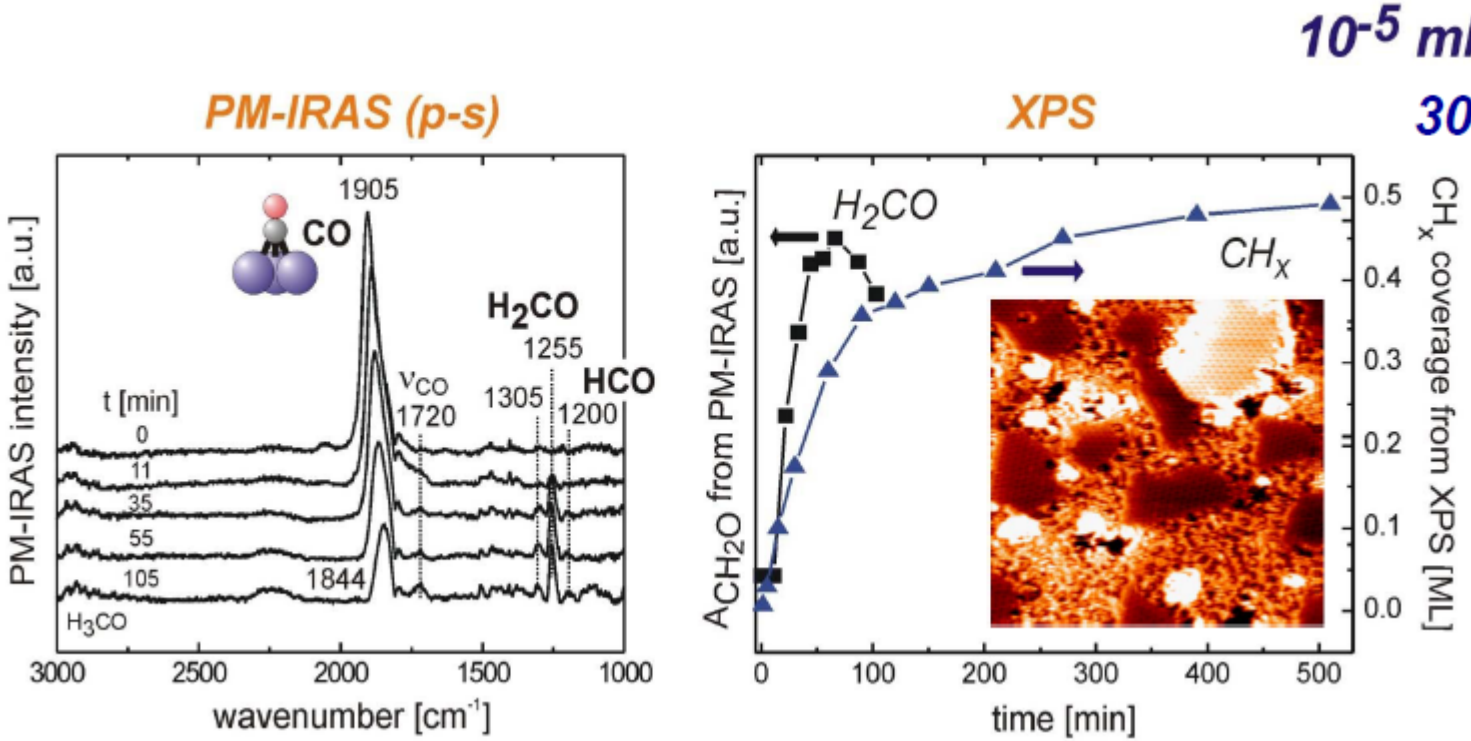

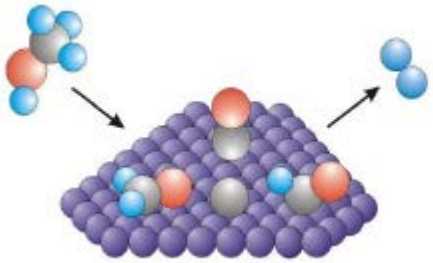

CH_x seems to stabilize CH_2O

G. Rupprechter, C. Weilach, J. Phys.: Condens. Matter 20 (2008) 184019

Methanol oxidation on Pd(111) and Pd nanoparticles on Al_2O_3/NiAl(110)

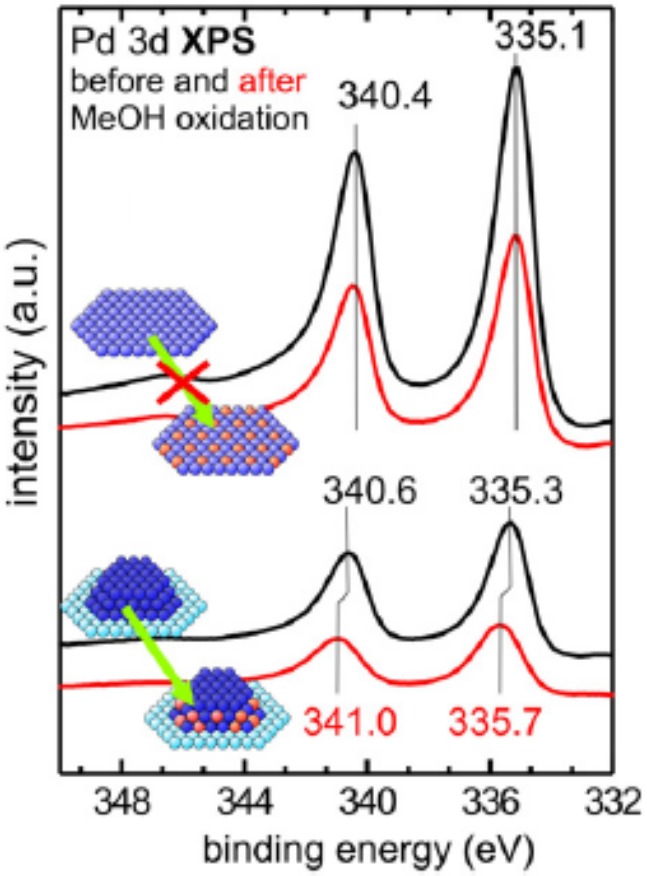

metallic on Pd(111)

Ox on nanoparticles (6 nm): partial oxidation
ring reaction at 400 K

G. Rupprechter, C. Weilach, J. Phys.: Condens. Matter 20 (2008) 184019

Reaction mechanism

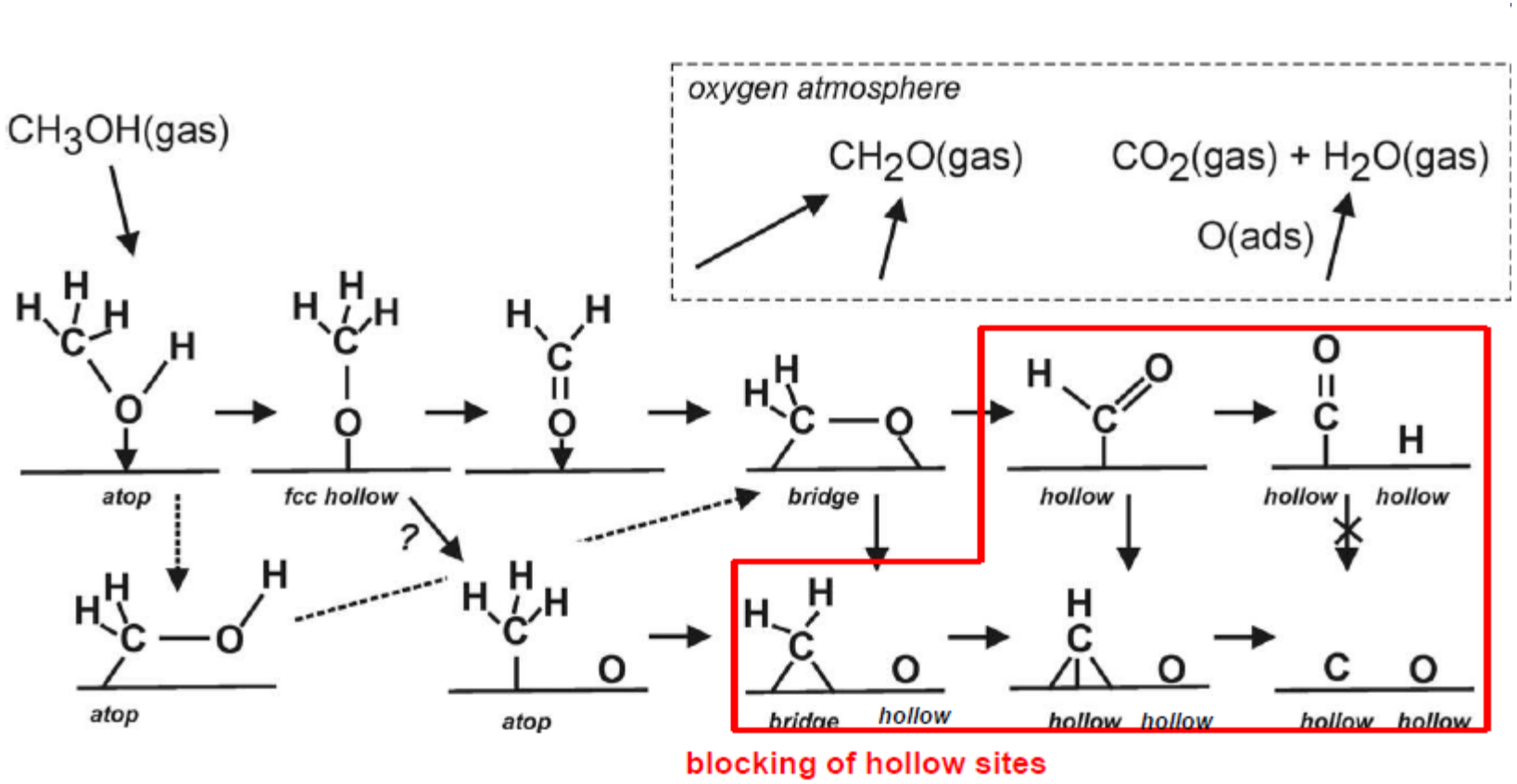

Literature

I. Chorckendorff, J.W. Niemantsverdriet, „Concepts of Modern Catalysis and Kinetics“, Wiley-VCH 2003.

R. I. Masel, „Chemical Kinetics and Catalysis“, Wiley 2001.

R. A. van Santen, J. W. Niemantsverdriet, „Chemical Kinetics and Catalysis“, Plenum 1995.

G. Ertl, H. Knözinger, F. Schüth, J. Weitkamp, (Eds.), „Handbook of Heterogeneous Catalysis“, 2nd ed., Wiley-VCH 2008.

J. W. Niemantsverdriet, „Spectroscopy in Catalysis“, Wiley-VCH 2000.

K. Oura et al., „Surface Science“, Springer 2003.

H. Lüth, „Solid Surfaces, Interfaces and Thin Films“, Springer 2001.